Journal of Experimental Systems

Journal of Experimental Systems

Definition of the Journal

Scientific Objectives

To support the International Scientific Community in its written production of Science, Technology and Innovation in the area of Biology and Chemistry, in the sub-disciplines of analytical chemistry, pharmaceutical chemistry, physical chemistry, inorganic chemistry, macromolecular chemistry, nuclear chemistry, fluid physics, physics, statistics, molecular physics, theoretical physics.

ECORFAN-Mexico S.C. is a Scientific and Technological Company contributing to the formation of Human Resources focused on the continuity in the critical analysis of International Research and is attached to the RENIECYT of CONAHCYT with number 1702902, its commitment is to disseminate research and contributions of the International Scientific Community, academic institutions, agencies and entities of the public and private sectors and contribute to the linkage of researchers who carry out scientific activities, technological developments and training of specialized human resources with governments, businesses and social organizations.

Encourage the dialogue of the International Scientific Community with other study centres in Mexico and abroad and promote a wide incorporation of academics, specialists and researchers to the serial publication in Science Niches of Autonomous Universities - State Public Universities - Federal HEIs - Polytechnic Universities - Technological Universities - Federal Technological Institutes - Teacher Training Colleges - Decentralised Technological Institutes - Intercultural Universities - S&T Councils - CONAHCYT Research Centres.

Scope, Coverage and Audience

Revista de Sistemas Experimentales is a Journal edited by ECORFAN-México S.C. in its Holding with repository in Bolivia, it is a refereed and indexed scientific publication with quarterly periodicity. It admits a wide range of contents that are evaluated by academic peers by the double-blind method, on topics related to the theory and practice of analytical chemistry, pharmaceutical chemistry, physical chemistry, inorganic chemistry, macromolecular chemistry, nuclear chemistry, fluid physics, physics, statistics, molecular physics, theoretical physics with diverse approaches and perspectives, which contribute to the dissemination of the development of Science, Technology and Innovation that allow the arguments related to decision-making and influence the formulation of international policies in the field of Biology and Chemistry. The editorial horizon of ECORFAN-Mexico® extends beyond academia and integrates other segments of research and analysis outside that field, as long as they meet the requirements of argumentative and scientific rigour, in addition to addressing issues of general and current interest of the International Scientific Society.

Arbitration Committee

Assignment of Rights

The submission of an article to the Journal of Experimental Systems implies the author's commitment not to submit it simultaneously to the consideration of other serial publications. To do so, he/she must complete the Originality Form for his/her article.

The authors sign the Authorisation Form for their article to be disseminated by the means that ECORFAN-Mexico, S.C. in its Holding Bolivia considers pertinent for the dissemination and diffusion of their article, ceding their copyright.

Declaration of Authorship

Indicate the name of 1 author and a maximum of 3 co-authors in the participation of the article and indicate in full the Institutional Affiliation indicating the Unit.

Identify the name of 1 author and a maximum of 3 co-authors with the CVU number -PNPC or SNI-CONACYT- indicating the level of researcher and their Google Scholar profile to verify their citation level and H index.

Identify the Name of 1 Author and 3 Co-authors maximum in the Science and Technology Profiles widely accepted by the International Scientific Community ORC ID - Researcher ID Thomson - arXiv Author ID - PubMed Author ID - Open ID respectively.

Indicate the contact for correspondence to the Author (Mail and Telephone) and indicate the Contributing Researcher as the first Author of the Article.

Plagiarism Detection

All articles will be tested by the PLAGSCAN plagiarism software. If a positive plagiarism level is detected, the article will not be sent to arbitration and the receipt of the article will be rescinded, notifying the responsible authors, claiming that academic plagiarism is classified as a crime in the Penal Code.

Refereeing Process

All articles will be evaluated by academic peers using the Double Blind method. Approved refereeing is a requirement for the Editorial Board to make a final decision which will be final in all cases. MARVID® is a spin-off brand of ECORFAN® specialised in providing expert reviewers all of them with PhD degree and distinction of International Researchers in the respective Councils of Science and Technology and the counterpart of CONAHCYT for the chapters of America-Europe-Asia-Africa and Oceania. The identification of authorship should only appear on a first page that can be removed, in order to ensure that the refereeing process is anonymous and covers the following stages: Identification of the Research Journal with its author occupancy rate - Identification of Authors and Co-authors - PLAGSCAN Plagiarism Detection - Review of Authorisation and Originality Formats - Assignment to the Editorial Board - Assignment of the pair of Expert Referees - Notification of Opinion - Declaration of Observations to the Author - Modified Article Package for Editing - Publication.

Instructions for Scientific, Technological and Innovation Publication Area of Knowledge

The works must be unpublished and refer to logical methods, research methods, hypothetical-deductive method, scientific observation method, measurement method, scientific experimentation, climatology, geology, geochemistry, acoustics and other topics related to Biology and Chemistry.

Presentation of the Content

As a first article we present *Synthesis and characterization of carbon-based quantum dots for use in biotechnology*, by Granados-Olvera, Jorge Alberto, Calvillo-Beltrán, Sofía Valentina, Arroyo-Ordoñez, Ivan and Rangel-Ruíz, Karelia Liliana, based at the Universidad Politécnica de Cuautitlán Izcalli. As next article we present *Biofilm of potato starch and silver nanoparticles*, by Díaz-Silvestre, Sergio E. & Ramirez, Leticia, with secondment to the Universidad Tecnológica de Coahuila. As next article we present *Solubility study of aerosols and vinyl paint on stone surfaces*, by García-Dorado, Samantha, Carranza-Téllez, José, Villegas-Martínez, Rodrigo and García-González, Juan Manuel, with secondment to the Universidad Autónoma de Zacatecas "Francisco García Salinas". As next article we present *Anticorrosive SiO₂-PDMS ceramic coating: effect of viscosity and functional group on the siloxane chain*, by Salazar-Hernández, Carmen, Salazar-Hernández, Mercedes, Mendoza-Miranda, Juan Manuel and Elorza-Rodríguez, Enrique, with secondment to the Instituto Politécnico Nacional-UPIIG and Universidad de Guanajuato. As next article we present *Optimization of the finite element meshing for the fabrication of a M3x12x0.5 screw, in 3D printing*, by González-Sosa, Jesús Vicente, Avila-Soler, Enrique and Zavala-Osorio, Yadira, with secondment to the Universidad Autónoma Metropolitana. As the last article we present, *SiO₂/PDMS modified porous systems for oil removal: reuse cycles* studied, by Salazar-Hernández, Carmen, Salazar-Hernández, Mercedes, Mendoza-Miranda, Juan Manuel and León-Reyes, María del Rosario, with secondment to the Instituto Politécnico Nacional-UPIIG and Universidad de Guanajuato.

Content

Article	Page

Synthesis and characterization of carbon-based quantum dots for use in biotechnology

Síntesis y caracterización de puntos cuánticos a base carbono para su uso en la biotecnología

Granados-Olvera, Jorge Alberto*[a], Calvillo-Beltrán, Sofía Valentina[b], Arroyo-Ordoñez, Ivan[c] and Rangel-Ruíz, Karelia Liliana[d]

[a] ROR Universidad Politécnica de Cuautitlán Izcalli • 🔹 S-5756-2018 • 🔸 0000-0003-0546-5328 • 🔹 946998
[b] ROR Universidad Politécnica de Cuautitlán Izcalli • 🔹 KYU-8461-2024 • 🔸 0009-0003-8078-7172 • 🔹 2052292
[c] ROR Universidad Politécnica de Cuautitlán Izcalli • 🔹 LBI-3522-2024 • 🔸 0009-0005-5151-5471 • 🔹 1196052
[d] ROR Universidad Politécnica de Cuautitlán Izcalli • 🔹 GLQ-8704-2022 • 🔸 0000-0003-1805-0447 • 🔹 225798

Abstract

Carbon quantum dots (CQDs) are spherical nanoparticles (CNPs) with a size between 2-10 nm and a crystalline structure. They have unique properties, such as high biocompatibility and luminescence produced by their absorbance and emission of light. This shows optical properties that are not seen in larger scale materials. Due to their low toxicity, CQDs offer a versatile platform for various applications, including medical diagnosis, bioimaging, substance detection, controlled drug release, photodynamic therapy and biomarking techniques. They can be synthesized by methods such as ultrasound and microwaves, pyrolysis, hydrothermal synthesis, or exfoliation of carbon materials. Their study and development is an active area of research in biotechnology, nanotechnology and materials science. This work focuses on the properties that this type of nanoparticle has, the synthesis used for its manufacture and the possible uses as a tool in different biotechnological processes.
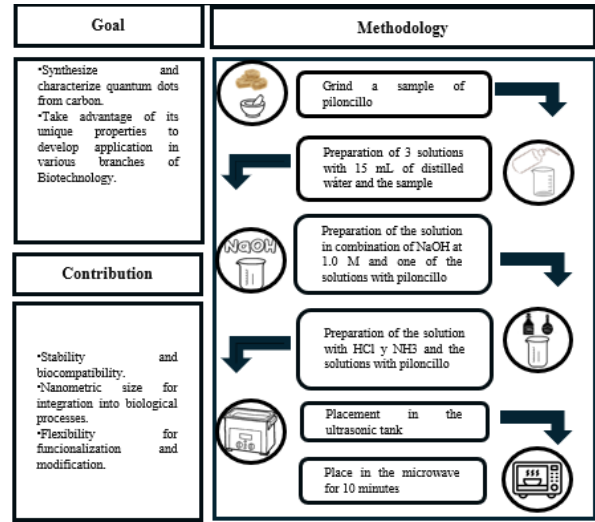
Resumen

Los puntos Cuánticos de carbono (CQDs) son nanopartículas de forma esférica (CNPs) con un tamaño entre 2-10 nm y una estructura cristalina. Cuentan con propiedades únicas, como elevada biocompatibilidad y luminiscencia producida por su absorbancia y emisión de luz. Lo que exhibe propiedades ópticas que no se observan en materiales a mayor escala. Debido a su baja toxicidad los CQDs ofrecen una plataforma versátil para diversas aplicaciones, incluyendo diagnóstico médico, bioimagen, detección de sustancias, liberación controlada de fármacos, terapia fotodinámica y técnicas de biomarcaje. Pueden ser sintetizados mediante métodos como ultrasonido y microondas, pirólisis, síntesis hidrotermal o exfoliación de materiales de carbono. Su estudio y desarrollo es un área activa de investigación en biotecnología, nanotecnología y ciencia de materiales. El presente trabajo se enfoca en las propiedades que este tipo de nanopartícula posee, la síntesis usada para su fabricación y los posibles usos como herramienta en los diferentes procesos biotecnológicos.

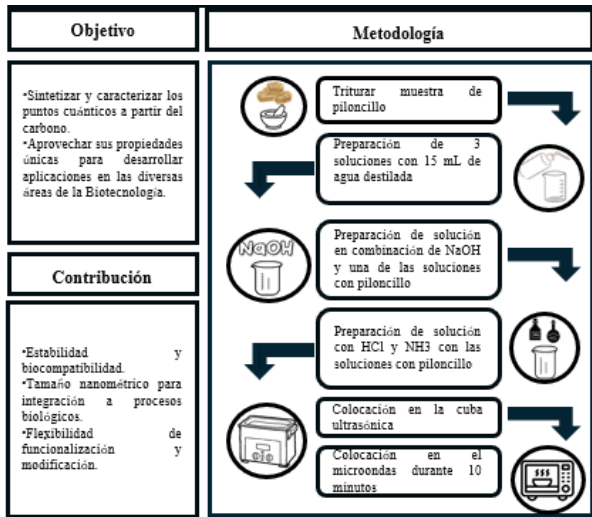| Goal	Methodology
•Synthesize and characterize quantum dots from carbon. •Take advantage of its unique properties to develop application in various branches of Biotechnology.	Grind a sample of piloncillo → Preparation of 3 solutions with 15 mL of distilled water and the sample → Preparation of the solution in combination of NaOH at 1.0 M and one of the solutions with piloncillo → Preparation of the solution with HCl y NH3 and the solutions with piloncillo → Placement in the ultrasonic tank → Place in the microwave for 10 minutes
Contribution	
•Stability and biocompatibility. •Nanometric size for integration into biological processes. •Flexibility for funcionalization and modification.	

Objetivo	Metodología
•Sintetizar y caracterizar los puntos cuánticos a partir del carbono. •Aprovechar sus propiedades únicas para desarrollar aplicaciones en las diversas áreas de la Biotecnología.	Triturar muestra de piloncillo → Preparación de 3 soluciones con 15 mL de agua destilada → Preparación de solución en combinación de NaOH y una de las soluciones con piloncillo → Preparación de solución con HCl y NH3 con las soluciones con piloncillo → Colocación en la cuba ultrasónica → Colocación en el microondas durante 10 minutos
Contribución	
•Estabilidad y biocompatibilidad. •Tamaño nanométrico para integración a procesos biológicos. •Flexibilidad de funcionalización y modificación.	

Synthesize, Characterization, Quantum dots

Síntesis, Caracterización, Puntos cuánticos

Article

Introduction

Quantum dots (QDs) are small semiconductor nanoparticles (NPs) of 2 to 10 nanometers (nm) in diameter. They are composed of various materials, including semiconductors, metals and carbon. They typically contain only 100,000 atoms and have a well-defined crystalline structure, allowing them to reveal unique optical and electronic properties (Tao et al., 2019).

They possess qualities such as electron confinement, energy quantization and the ability to absorb and emit light at different wavelengths depending on their composition and size. Furthermore, due to their tiny size, QDs suffer several quantum effects such as the discretization of their energy bands. Under these characteristics, QDs can interact with light and matter differently than materials on a larger scale; this is due to the quantum confinement effect, which occurs when particles are so small that electrons behave differently due to energy quantization. Quantum confinement occurs when the diameter of the crystal is smaller than its Bohr radius and influences the properties of the QDs to be quite different from those of macroscopic materials (B.H. Juárez, 2011).

An attractive property of these NPs is that they show confinement in the three directions of space; this is because the electrons are restricted to move in extremely small regions, less than 10 nm.

QDs can be considered nanocrystalline due to their crystalline structure and nanometric size; and since they are made up of semiconductor materials, they have a valence band (saturated with electrons) and a conduction band (empty energy band) separated by an energy difference called a gap.

The luminescent process in quantum dots occurs through the emission of light when electrons relax from a higher energy state to a lower energy state. This process consists of four stages, excitation, relaxation, emission and recombination. During the excitation phase, the QDs absorb the energy of incident light, which excites the electrons in the valence band and leads them to a higher energy state in the conduction band, leaving gaps in the Valence band.

When the excitation phase ends, the relaxation phase begins; in this phase the electrons in the state of higher energy are relaxed toward the lowest energy state, releasing the excess of this in the form of light generated as a radiative combination between the generated electrons and holes, causing the emission of photons with a defined energy. This gives way to the emission phase, where the emitted light has a specific wavelength, which depends on the size and composition calculated by the separation between the two energy levels. Finally, the recombination phase is reached, in which electrons and gaps recombine, releasing excess energy in the form of light (Cui et al., 2018).

The importance of knowledge of quantum dots lies in their potential to be used in a variety of biotechnological applications such as bioimaging, photodynamic therapy, drug administration, medical diagnosis, genetic applications, bioassays, biosensor development, among others. In addition to their applications, they can enhance understanding of different biological processes to develop new tools and technologies for creating smaller and more efficient devices and materials, while promoting understanding of quantum physics and its applications in engineering.

The added value of quantum dots development in the present work is the use of carbon as a basis; as it is more sustainable compared to its manufacture with other materials, as they can be produced from renewable sources of carbon. This feature makes them biocompatible and of low toxicity, without losing their chemical stability, resulting in a great resistance in aggressive environments and endowing them with a great versatility, as they can be functionalized with different chemical groups. Not to mention that its profitability is quite attractive, as it is considerably lower compared to other materials.

The present work seeks to obtain the optimal conditions for the synthesis and characterization of carbon-based QD for IR and UV-VIS tests to analyse the scope of these possess and taking that into account consider what uses could give them for their implementation in the biotechnological area.

Journal of Experimental Systems

Article

Background

The term quantum dots is mainly associated with nanoparticles with diameters less than 10 nm, typically based on a metal and a nonmetal (commonly group 15 or 16), which show different optical properties not only from macroscopic materials, but also from corresponding nanoparticles with sizes greater than 10 nm (Murray et al., 2000). This is due to electronic confinement (also called quantum confinement) due to the small particle size (Ashoori, 1996), which for this type of materials results in photon absorption typical in the near UV or the visible and strong emission (high quantum yield – ratio of photons emitted between those absorbed) adjustable throughout the visible range. Semiconductor quantum dots were discovered in 1980 by two independent groups, one in Russia by Alexei I. Ekimov in a glass array; and the other in the United States of America by Louis E. Brus and Alexander Afros who obtained them in colloidal solutions (Akimov & AMP; Anshchenko, 2023).

Currently, they are being researched for electro-optical applications such as photovoltaic devices (such as dyes absorbing sunlight), light-emitting diodes (already with commercial applications such as their use in QLED televisions, for example), photosensing, photocatalysis and bioimaging (as an alternative to traditional stains for fluorescent microscopy) (Bera et al., 2010; Kairdolf et al., 2013; Martynenko et al., 2017).

The range of applications for quantum dots is wide, however, there are concerns about the effect on health and the environment with the use and disposal of these materials which include metal ions such as Cd^{2+}, Pb^{2+} as well as some non-metals such as As^{3-}, Se^{2-}, and Te^{2-} considered toxic (Filali et al., 2020; Hardman, 2006).

From this point lies the interest in less dangerous alternatives, such as carbon-based quantum dots (CQDs). These were discovered in 2004 when researchers purified the soot residue of arc flash by synthesizing carbon nanotubes and noticed unexpected fluorescent properties (Xu et al., 2004).

Since that study to date, there has been great progress in the scientific community that seeks to replace inorganic quantum dots with carbon quantum dots that can provide similar properties with simple syntheses, at low cost, using widely available precursors, with easy waste management, lower toxicity and greater biocompatibility, for use in areas of medicine and energy mainly.

Synthesis of CQDs

The synthesis of CQDs tends to include a breakdown, polymerization, and carbonization of molecules. Normally this process occurs in some aqueous medium, so the final functional groups on the surface of CQDs are hydrophilic (Cayuela et al., 2016).

In the present paper the CQDs were synthesized using an organic precursor; piloncillo, this contains carbohydrates such as sucrose, glucose and fructose. This means that it has functional groups such as -OH and -CO; these groups can dehydrate at high temperatures, which is why it was decided to carry out this synthesis by ultrasound and microwave. This process by which synthesis is carried out is called sonication, and the type of chemistry used in this technique is known as Sonochemistry (Dong et al., 2013).

Methodology

The synthesis of quantum points of carbon was carried out using a green synthesis taking as a precursor the glucose from the piloncillo, a base of Sodium Hydroxide (NaOH), Hydrochloric Acid (HCl) and an ammonia base (NH_3), thus obtaining a homogeneous solution (Figure 1).

Box 1

Figure 1

Homogeneous solutions with piloncillo as a precursor and base of NH_3 (right vessel), NaOH (medium vessel) and HCl (left vessel)

Source: Own elaboration

The sample is crushed with the help of a mortar until a fine powder is obtained from it, subsequently 3 solutions were prepared in which they were mixed at 1.0 M of the respective powder, using this unique concentration for the 3 different solutions with 30 mL of distilled water each, consequently they were stirred to obtain a homogeneous mixture with the piloncillo respectively.

Once prepared the solutions with distilled water and the sample were subjected to the ultrasonic cube for a period of 30 minutes (Figure 2).

Box 2

Figure 2

Solutions subjected to ultrasonic cleaning

Source: Own elaboration

The solutions were subsequently prepared with NaOH, HCl and NH3. For the NaOH solution, 30 mL of distilled water and one 1.0 M solution were used, for the HCl and NH3 solution, a combination of 30 ml of distilled water and a 30% V-V solution was used, and the solutions were shaken until they were completely diluted.

To complete this process, the homogeneous mixture of piloncillo is placed in a precipitated jar and the precursor solutions are added to it (Figure 3), again the mixtures are shaken for 15 minutes, subsequently exposed for 30 minutes to the ultrasonic cube and finally subjected to microwave for 7 minutes at a power of 10 Watts.

Box 3
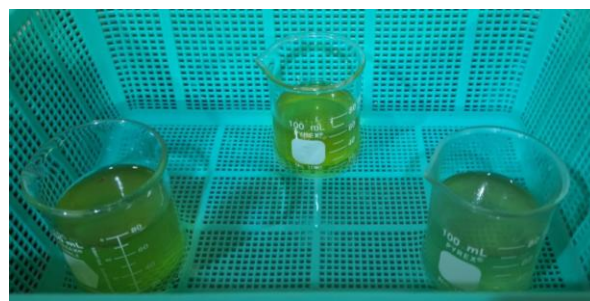
Figure 3

Precursor solution with homogenized base solution and NH3 (right vessel), NaOH (medium vessel) and HCl (left vessel)

Source: Own elaboration

Results

Box 4

Figure 4

CQDs with UV exposure

Source: Own elaboration

Uv-vis spectroscopy

The different solutions contained in the CQDs were exposed to ultraviolet light radiation, to visually check for luminescent properties. Figure 4 shows samples obtained from CQDs with and without ultraviolet radiation where the presence of luminescent properties is confirmed.

The aquatic solutions of quantum dots have their maximum excitation at 341 nm within the ultraviolet spectrum and an emission close to 442 nm inside the visible range in a cyan-blue color.

Granados-Olvera, Jorge Alberto, Calvillo-Beltrán, Sofía Valentina, Arroyo-Ordoñez, Ivan and Rangel-Ruíz, Karelia Liliana. [2024]. Synthesis and characterization of carbon-based quantum dots for use in biotechnology. Journal of Experimental Systems. 11[30]-1-7: e11130107.
DOI: https://doi.org/10.35429/JOES.2024.11.30.1.7

From the spectroscopes it is observed that the intensity of luminescence depends on the increase in the concentration of organic material (Figure 5) until it reaches an over-saturation in concentration and has a decrease in intensity due to a phenomenon called cooling of concentration, on the other hand, the luminescent intensity will depend on the reaction time.

Box 5
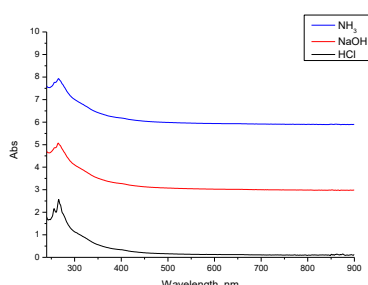
Figure 5

UV-Visible Spectrum of Quantum Carbon Dots

Source: Own elaboration

UV-Visible spectra show wide absorption at 280 nm (Figure 5) which is consistent with what is in various research (A. Mewada, 2013).

The quantum carbon dots have absorption bands at 250 and 280 nm, (Figure 2), which correspond to the bond and transition π-π^* between carbon atoms C=C of aromatic domains, such absorptions are attributed to the n- π transition of the bands C=O and C = C. On the other hand, an absorption at 280 nm is observed indicating the presence of carbon nanoparticles.

FT-IR spectroscopy

Infrared spectroscopy was used to identify functional groups present in the carbon quantum points of the representative samples. IR spectroscopes (Figure 6) show absorption bands present at 3339, 2118, 1627 and 1159 at 1021 cm-1, indicating the existence of functional groups OH-, C-H, C-N, C=C and C-O, C-OH, C -O-C, COOH, C = C (Valencia, 2019).

From these results the quantum carbon dots obtained from piloncillo are composed of multiple functional groups which makes them highly soluble in water and makes them good candidates for their application in biotechnology.

Box 6
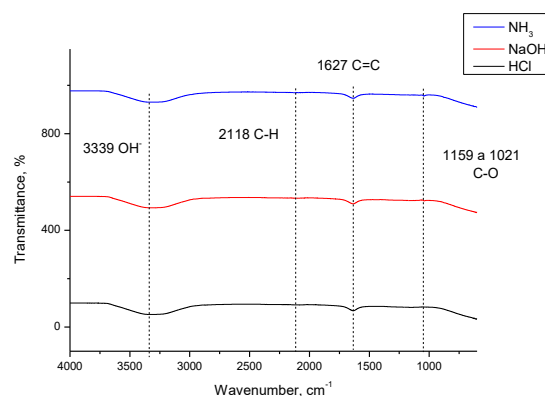
Figure 6

FT-IR spectrum of Quantum Carbon Dots

Source: Own elaboration

Another variable to which the maximum intensity is attributed is to concentration; where at lower concentrations greater intensity, because at less matter, there is greater number of interactions for the formation of quantum dots. (Metha, 2014).

Conclusion

Quantum carbon dots were synthesized, with different solvents, obtained from piloncillo, which are cost-effective for their low cost of synthesis and environmentally friendly. Optimal emission conditions were found at a concentration of 0.1M in a time of 3 hours, presenting a maximum excitation at 280 nm, which will allow surface passivation for anchoring with biomolecules for application in biotechnology.

According to the FTIR analysis, the functional groups OH-, C-H, C-N, C = C and C-O, C - OH, C – O-C, COOH, C=C are identified as responsible for the functionalization of the surface that allowed the obtaining of luminescent properties (blue emission when excited by ultraviolet light with a wavelength of 254 nm).

Granados-Olvera, Jorge Alberto, Calvillo-Beltrán, Sofía Valentina, Arroyo-Ordoñez, Ivan and Rangel-Ruíz, Karelia Liliana. [2024]. Synthesis and characterization of carbon-based quantum dots for use in biotechnology. Journal of Experimental Systems. 11[30]-1-7: e11130107.
DOI: https://doi.org/10.35429/JOES.2024.11.30.1.7

Declarations

Conflict of interest

The authors declare no interest conflict. They have no known competing financial interests or personal relationships that could have appeared to influence the article reported in this article.

Authors' Contribution

The contribution of each researcher in each of the points developed in this research, was defined based on:

Granados-Olvera, Jorge Alberto: Contributed to the project conception, research method and synthesis. He performed the analysis of results and the characterization of quantum dots, as well as the writing of the article.

Calvillo-Beltrán, Sofía Valentina: Conducted the synthesis of quantum dots and collaborated in the development of graphs for the evaluation of results. She also contributed to the drafting of the article.

Arroyo-Ordoñez, Ivan: Contributed to the development of the research and the introduction, the type of quantum dots and the results collection. He also helps with the approached and the writing of the article.

Rangel-Ruíz, Karelia Liliana: Worked on the search for applications of quantum dots in the biotechnology area and on data collection. She also collaborated in the writing of the document.

Availability of data and materials

The availability of materials is quite wide, and they are in the industrial category due to since the precursor, in this case piloncillo, can be easily obtained in different grocery stores. The equipment used for the Sonochemical technique is inexpensive compared to other methods and gives optimal results. The data, on the other hand, were obtained from the spectra and graphed with a program.

Funding

The research did not receive any funding.

Abbreviations

CNPs: Core-Shell Nanoparticles

CQDs: Carbon Quantum Dots

nm: Nanometer

NPs: Nanoparticles

QDs: Quantum Dots

UV-vis: Visible ultraviolet

References

Antecedents

Dong, Y., Pang, H., Yang, H. B., Guo, C., Shao, J., Chi, Y., Li, C. M., & Yu, T. (2013). Carbon-Based Dots Co-doped with Nitrogen and Sulfur for High Quantum Yield and Excitation-Independent Emission. *Angewandte Chemie International Edition*, *52*(30), 7800-7804. https://doi.org/10.1002/anie.201301114

Supports

Cayuela, A., Carrillo-Carrión, C., Soriano, M. L., Parak, W. J., & Valcárcel, M. (2016). One-Step Synthesis and Characterization of N-Doped Carbon Nanodots for Sensing in Organic Media. *Analytical Chemistry*, *88*(6), 3178-3185. https://doi.org/10.1021/acs.analchem.5b04523

Mehta, V. N., Jha, S., Singhal, R. K., & Kailasa, S. K. (2014). Preparation of multicolor emitting carbon dots for HeLa cell imaging. *New J. Chem.*, *38*(12), 6152-6160. https://doi.org/10.1039/C4NJ00840E

Murray, C. B., Kagan, C. R., & Bawendi, M. G. (2000). Synthesis and Characterization of Monodisperse Nanocrystals and Close-Packed Nanocrystal Assemblies. *Annual Review of Materials Science*, *30*(1), 545-610. https://doi.org/10.1146/annurev.matsci.30.1.545

Xu, X., Ray, R., Gu, Y., Ploehn, H. J., Gearheart, L., Raker, K., & Scrivens, W. A. (2004). Electrophoretic Analysis and Purification of Fluorescent Single-Walled Carbon Nanotube Fragments. *Journal of the American Chemical Society*, *126*(40), 12736-12737. https://doi.org/10.1021/ja040082h

Zamora Valencia, C. A., Reyes Valderrama, M. I., Herrera Carbajal, A. D. J., Salinas Rodríguez, E., & Rodriguez Lugo, V. (2019). Evaluación de la lumiscencia de puntos cuánticos de carbono sintetizados mediante el método hidrotermal a partir de triticum. *Pädi Boletín Científico de Ciencias Básicas e Ingenierías del ICBI*, *7*(Especial-2), 19-22. https://doi.org/10.29057/icbi.v7iEspecial-2.4745

Discussions

Ashoori, R. C. (1996). Electrons in artificial atoms. *Nature*, *379*(6564), 413-419. https://doi.org/10.1038/379413a0

Bera, D., Qian, L., Tseng, T.-K., & Holloway, P. H. (2010). Quantum Dots and Their Multimodal Applications: A Review. *Materials*, *3*(4), 2260-2345. https://doi.org/10.3390/ma3042260

Cui, B., Yan, L., Gu, H., Yang, Y., Liu, X., Ma, C.-Q., Chen, Y., & Jia, H. (2018). Fluorescent carbon quantum dots synthesized by chemical vapor deposition: An alternative candidate for electron acceptor in polymer solar cells. *Optical Materials*, *75*, 166-173. https://doi.org/10.1016/j.optmat.2017.10.010

Ekimov, A. I., & Onushchenko, A. A. (2023). Quantum Size Effect in Three-Dimensional Microscopic Semiconductor Crystals. *JETP Letters*, *118*(S1), S15-S17. https://doi.org/10.1134/S0021364023130040

Filali, S., Pirot, F., & Miossec, P. (2020). Biological Applications and Toxicity. Minimization of Semiconductor Quantum Dots. *Trends in Biotechnology*, *38*(2), 163-177. https://doi.org/10.1016/j.tibtech.2019.07.013

Hardman, R. (2006). A Toxicologic Review of Quantum Dots: Toxicity Depends on Physicochemical and Environmental Factors. *Environmental Health Perspectives*, *114*(2), 165-172. https://doi.org/10.1289/ehp.8284

Kairdolf, B. A., Smith, A. M., Stokes, T. H., Wang, M. D., Young, A. N., & Nie, S. (2013). Semiconductor Quantum Dots for Bioimaging and Biodiagnostic Applications. *Annual Review of Analytical Chemistry*, *6*(1), 143-162. https://doi.org/10.1146/annurev-anchem-060908-155136

Martynenko, I. V., Litvin, A. P., Purcell-Milton, F., Baranov, A. V., Fedorov, A. V., & Gun'ko, Y. K. (2017). Application of semiconductor quantum dots in bioimaging and biosensing. *Journal of Materials Chemistry B*, *5*(33), 6701-6727. https://doi.org/10.1039/C7TB01425B

Tao, S., Feng, T., Zheng, C., Zhu, S., & Yang, B. (2019). Carbonized Polymer Dots: A Brand New Perspective to Recognize Luminescent Carbon-Based Nanomaterials. *The Journal of Physical Chemistry Letters*, *10*(17), 5182-5188. https://doi.org/10.1021/acs.jpclett.9b01384

Article

Biofilm of potato starch and silver nanoparticles

Biopelícula de almidón de papa y nanopartículas de plata

Díaz-Silvestre, Sergio E.*[a] & Ramirez, Leticia[b]

[a] ROR Universidad Tecnológica de Coahuila • ᴄ LBH-9981-2024 • 0000-0002-6765-3415 • 334151
[b] ROR Universidad Tecnológica de Coahuila • ᴄ LBH-6830-2024 • 0009-0009-7093-0813 • 511901
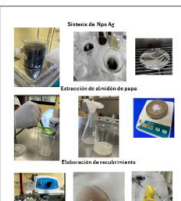
Abstract

The biofilm and covering have been used to promote the change and improve the natural peel of diverse fruits, to prevent the loss of humidity, to allow the interchange of gases, to provide sterility and conservation. Therefore, in recent years a growing interest in the organic films has emerged, this organic films are very diverse, highlighting the potato starch based biofilms. In this investigation some silver nanoparticles were synthesized by the chemical reduction process and were used as covering in fruits to avoid the growing of bacteria in strawberry and apples in conditions of room temperature to maximize the lifetime in shelf of this perishable fruits.

Synthesis, Silver nanoparticles, Nanocoating

Resumen

Las películas y recubrimientos se han empleado para promover el reemplazo y reforzar las capas naturales de diversos frutos, para prevenir la perdida de humedad, permitir el intercambio de gases, proporcionar esterilidad y la conservación. Por lo tanto, en los últimos años ha surgido un creciente interés en las películas de origen orgánico, las cuales pueden ser muy variadas, destacando las biopelículas a base de almidón de papa. En este trabajo se sintetizaron nanopartículas de plata mediante el proceso de reducción química las cuales fueron usadas como recubrimientos para frutas y así evitar el crecimiento bacteriano en frutas como la fresa y la manzana a temperatura ambiente para maximizar la vida de anaquel de estos perecederos.

Síntesis, Nanopartículas de plata, Nanorecubrimiento

Introduction

The biofilm and covering have been used to promote the replace and strengthen the natural peel of diverse fruits, to prevent the loss of humidity, to allow the interchange of gases, to provide sterility and to preserve the fruits. (Torrenegra 2016; Vazquez-Ovando,2013) In recent years a growing interest in the organic films has risen, this films are very diverse, specially the biofilms based in potato starch which stand out from others. (Reyes, 2019)

This product can be used to manufacture of bioplastics derivate from alternative compounds instead of petroleum with a lower impact in the environment with their production contributing to the climate change. (Cortez-Mazatan, 2011)

The use of nanotechnology to prolong the lifetime of the fruits and reduce the loss during these are transported, is an innovative concept for the food industry. Is expected that the nanomaterials will have a high impact in the development of the society. For this the application of the nanotechnology in the food conservation, like fruits, is innovative and with a high potential to improve the food safety and reduce the food waste. (Lira-Saldívar 2018)

The development of nano-biofilm to conserve fruits using nanomaterials is considered highly innovative. The application of nanotechnology in the food industry to solve conservation problems and food quality is a new approach with a high potential to impact the society and the food supply chain. (Lopez, 2020)

The nanomaterials are characterized to have dimensions in an atomic scale or in the range of 1 to 100 nanometers. This dimensions could give remarkable and significant properties in comparison with bulk materials.

Some of the nanomaterials properties, like the surface area, the spatial confinement and the reduction of imperfections give them a significant potential of innovation in different applications. The study of metallic nanoparticles has a high interest due to the possible applications from the optoelectronics to medical science, highlighting the silver nanoparticles in the case of medical science due to antimicrobial properties. (Nazario-Naveda, 2022; lopez-Carrizales, 2022)

The project is focused in apply nanotechnology to conserve of fruits, specifically strawberries and apples. The use of nano-biofilms based on potato starch and silver nanoparticles to coat this fruits has the purpose of keep the freshness and optimize the lifetime.

Methodology

The project was focused in the development of a nano-biofilm based on potato starch doped with silver nanoparticles to use in the conserve of fruits, especially strawberry and apples. The objective of this application is to extend the lifetime of these fruits and reduce the loss and waste while transport and storage.

Synthesis of silver nanoparticles

The synthesis was done using the chemical reduction method the $AgNO_3$ at 1M dissolved in water was used as precursor, the solution was agitated at constant temperature, when the 100°C was reached $Na_3C_6H_5O_7$ was added to the solution. Subsequently the temperature and agitation were constant of 1 hour, after the solution was filtered and send to dry at 60°C for 24 hours.

Coating application

The fruits were obtained with a state of maturity, these where selected to keep free of any defect that could affect the result of the coating. The fruits were washed, dried and storage at room temperature.

The microbial activity was observed with the use of an optical microscope.

Results

A nano-biofilm was elaborated using potato starch, with silver nanoparticles incorporated. In Figure 1 you can see the scanning electron microscopy (sem) analysis in which you can observe the good dispersion of the nanoparticles with a polymer matrix, showing the growth axis of the almost spherical crystals. It is important to say that with this technique only 2 micrometer particles could be observed since this was the first analysis and better characterization technologies are contemplated, as is observed in the figure 2
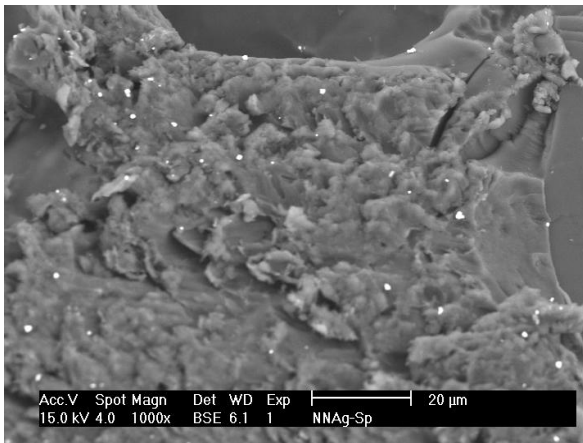
Díaz-Silvestre, Sergio E. & Ramirez, Leticia. [2024]. Biofilm of potato starch and silver nanoparticles. Journal of Experimental Systems. 11[30]-1-5: e21130105.
DOI: https://doi.org/10.35429/JOES.2024.11.30.1.5

Box 1

Figure 1

SEM image of the dispersion of silver nanoparticles in potato starch
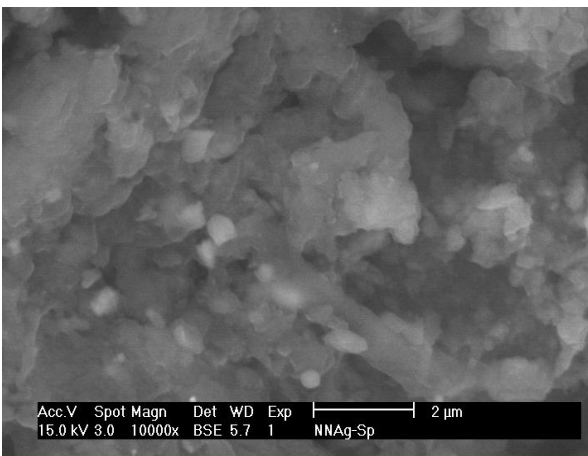
Box 2

Figure 2

SEM image of the morphology of silver nanoparticles in potato starch

By infrared spectroscopy technique it could be observed the different caracteristic signals for starch. The wave length gap of 3000-3900cm^{-1} corresponds to the OH group, in the 2000-2850cm^{-1} gap is the corresponding for C-H strain. There are also typical signals for C-O straining in the 1251-1255cm^{-1} gap, this corresponds to what Figueroa and collaborators have reported in 2016 when they made the corresponding to potatoe starch characterization, as is observed in the figure 3.
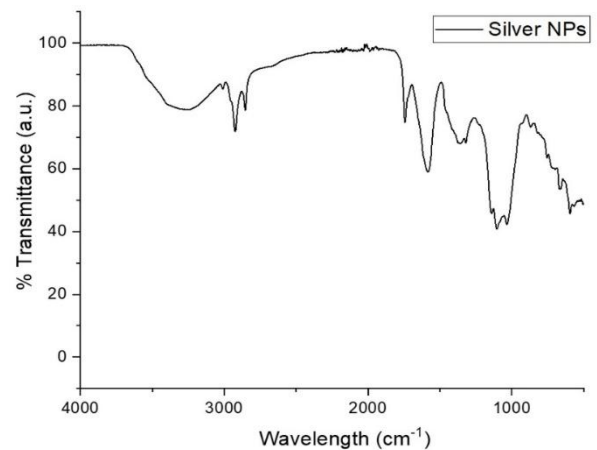
Box 3

Figure 3

Infrared spectrum of potato starch samples doped with silver nanoparticles

Source: [Origin 2018]

Coating on strawberry

The strawberries were covered with the nano-bioparticle developed and it was compared with strawberries without coating, during a period of 14 days at room temperature. The experiment was monitored by a series of photographs of both samples. In the figure 2 it could be observed a comparative of the products along the specified time observing that after 4 days the sample with coating had a good appearance while the sample without coating developed fungus after 3 days. It was observed with an optical microscope that the fruit with nano-biofilm coating showed a better conservation. The film acted like a barrier that retarded the growth of bacteria and fungus, extended the lifetime of the strawberries, as is observed in the figure 4.
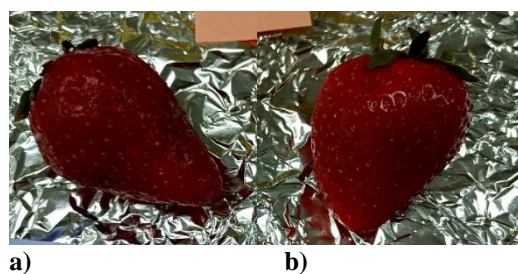
Box 4

a)   b)

Figure 4

a) Strawberries without coating
b) Strawberries with nano-biofilm coating

With the optical microscope was observed that the strawberries covered with the nano-bioparticles present a better conservation.

The biofilm acted like a barrier that retarded the growth of bacteria and fungus, extended the lifetime of the strawberries, in the figure 5 it is observed the changes in the strawberries along 14 days.

Box 5
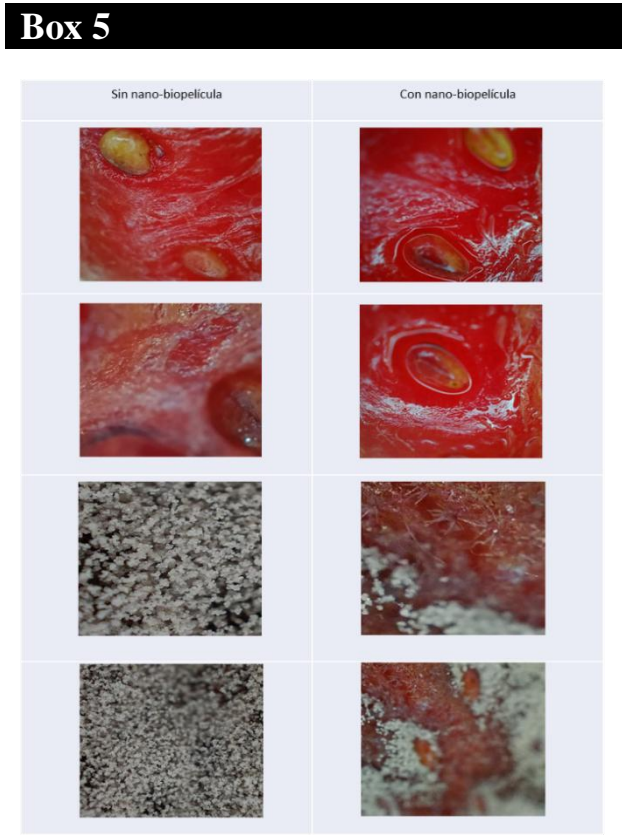
Figure 5

Monitoring of the strawberries using optical microscope

Coating on apples

The nano-biofilm was applied to apples to compare their appearance with apples without coating. The result shown that the apples with coating had an intense coloration and brightness in comparison with the non-coating apples.

Box 6

a)   b)
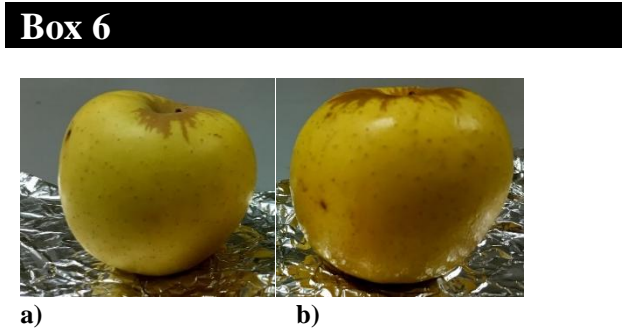
Figure 6

a) Apple without coating
b) Apple with coating

Through the monitoring performed with an optical microscope, some wáter drops were identified on the surface of the coated apples, it indicated the presence of nano-biofilm. It contributes to the improvement of the conservation of the apples.

Box 7
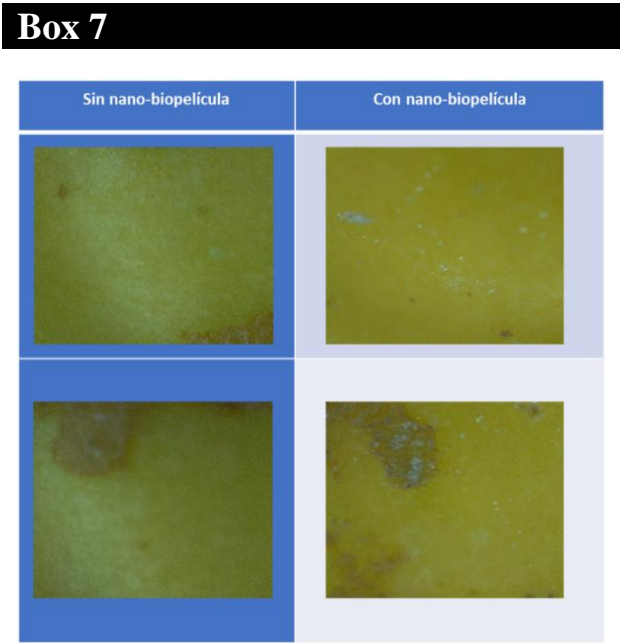
Figure 7

Monitoring of apples through optical microscope

The initial results shown a significant improvement in the time of conservation of both fruits when the nano-biofilm is applied. The presence of the film acted as a barrier that slow down the growth of bacteria and fungus, increasing the lifetime of the fruits.

Conclusions

The development of the nano-biofilm based in the potato starch and silver has demonstrated to be a solution in the conservation of strawberries and apples. With the passing of the test and improvements, this product has a potential to change the food industry with the reduction of losses during the transport and storage, it would contribute to satisfy the increasing demand of food in a constant growth market.

Declarations

Conflict of interest

The authors declare no interest conflict. They have no known competing financial interests or personal relationships that could have appeared to influence in this chapter.

Author contribution

Díaz-Silvestre, Sergio: Contributed to the project idea, bibliographic review and writing of the document.

Ramírez-Mendoza, Arizbeth: Contributed to the project idea, synthesis and characterization of nanoparticles, application and monitoring of nanobiocoating.

Abbreviations

SEM	sweep electronic microscopic analysis

References

Background

Torrenegra A, M., León M, G., Matiz M, G., Pájaro C, N., & Sastoque G, J. (2016). Evaluación de un biorecubrimiento comestible a base de almidon de ñame modificado. Revista Chilena de Nutricion: Organo Oficial de La Sociedad Chilena de Nutricion, Bromatologia y Toxicologia, 43(3), 8–8.

Alfredo Vázquez-Ovando Lourdes Adriano-Anaya Rosmeri Méndez-De León Salvador Figueroa Miguel. (2013). Elaboración y caracterización física de biorecubrimientos compuestos basados en quitosán. Quehacer Científico en Chiapas, 8(2013), 26–34.

Reyes Torres Uriel, (Diciembre 2019). Efecto de las nanopartículas de plata en la memoria de forma del almidón de papa termoplástico. Instituto Politécnico Nacional.

Cortez-Mazatán, G. Y., Valdez-Aguilar, L. A., Lira-Saldivar, R. H., & Peralta-Rodríguez, R. D. (2011). Polyvinyl acetate as an edible coating for fruits. Effect on selected physiological and quality characteristics of tomato. Revista Chapingo. Serie: Horticultura, XVII(1), 15–22.

Lira-Saldivar, R. H., Argüello, B. M., Villarreal, G. D. L. S., & Reyes, I. V. (2018). Potencial de la nanotecnología en la agricultura. Acta universitaria, 28(2), 9–24.

Basics

López, M. L. (23 de Octubre de 2020). Recubrimiento de Poli(Acetato De Vinilo-Co-Alcohol Vinílico) Adicionado con Nanopartículas de Óxido de Calcio y su Efecto en la Poscosecha de Pepino (Cucumis sativus). Centro de Investigación en Química Aplicada.

Support

Lopez-Carrizales, M., Pérez-Díaz, M. A., Mendoza-Mendoza, E., Peralta-Rodríguez, R. D., Ojeda-Galván, H. J., Portales-Pérez, D., Magaña-Aquino, M., Sánchez-Sánchez, R., & Martinez-Gutierrez, F. (2022). Green, novel, and one-step synthesis of silver oxide nanoparticles: antimicrobial activity, synergism with antibiotics, and cytotoxic studies. New Journal of Chemistry, 46(37), 17841–17853.

Differences

Nazario-Naveda, R., Delfin-Narciso, D., Juárez-Cortijo, L., Rojas Flores, S. J., Castillo-Ramírez, A., Chavín-Castillo, C., & Duran-Zambrano, M. (2022). Incorporation of biosynthesized silver nanoparticles in active biodegradable films of potato starch. Proceedings of the 20th LACCEI International Multi-Conference for Engineering, Education and Technology: "Education, Research and Leadership in Post-pandemic Engineering: Resilient, Inclusive and Sustainable Actions".

Article

Solubility study of aerosols and vinyl paint on stone surfaces

Estudio de solubilidad de aerosoles y pintura vinílica en superficies pétreas

García-Dorado, Samantha*[a], Carranza-Téllez, José[b], Villegas-Martínez, Rodrigo[c] and García-González, Juan Manuel[d]

[a] ROR Universidad Autónoma de Zacatecas "Francisco García Salinas"
[b] ROR Universidad Autónoma de Zacatecas "Francisco García Salinas" • 0009-0009-9805-4931
[c] ROR Universidad Autónoma de Zacatecas "Francisco García Salinas" • KZU-6876-2024 • 0000-0003-0474-6734
[d] ROR Universidad Autónoma de Zacatecas "Francisco García Salinas" • 0000-0001-7259-5021 • 346241
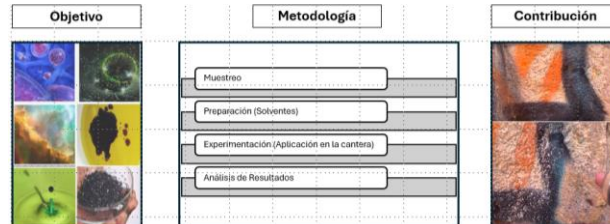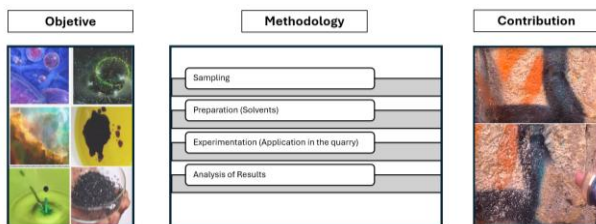
Abstract

Due to the existing needs, presented by the current state of conservation of the stone surfaces in ashlars of historic buildings in the city of Zacatecas, the conservation area of the INAH Zacatecas center will receive trained personnel to carry out the study of elements used in the removal of paint on stone surfaces, specifically pink quarry. This analysis seeks to provide solutions that allow the safeguarding of materials in conservation processes, facilitating the work to compensate for damages that are generated after anthropogenic activities of any kind. In the study, solutions were found that facilitate the elimination of products manufactured from alkenyl functional groups and acrylic functional groups, establishing the elimination parameters from pure substances and the elimination from specific colloidal systems.

Resumen

Debido a las necesidades existentes, que presenta el estado actual de conservación de las superficies pétreas en sillares de inmuebles históricos de la ciudad de Zacatecas, el área de conservación del centro INAH Zacatecas destino personal capacitado para llevar a cabo el estudio de elementos empleados en la eliminación de pinturas en superficies pétreas, específicamente cantera rosa. Se busca con este análisis se puedan dar soluciones, que permitan la salvaguarda de los materiales en los procesos de conservación, facilitando los trabajos de resarcimiento de daños que se generan tras actividades antropogénicas de cualquier índole. En el estudio se encontraron soluciones que facilitan la eliminación de productos fabricados a partir de los grupos funcionales alquenilos y los grupos funcionales acrilo, estableciendo los parámetros de eliminación a partir de sustancias puras y la eliminación a partir de sistemas coloidales específicos.

Objective	Methodology	Contribution
	Sampling	
	Preparation (Solvents)	
	Experimentation (Application in the quarry)	
	Analysis of Results	

Quarry, Solvent, Cleaning

Objetivo	Metodología	Contribución
	Muestreo	
	Preparación (Solventes)	
	Experimentación (Aplicación en la cantera)	
	Análisis de Resultados	

Cantera, Solvent, Limpieza

RENIECYT

Registro Nacional de Instituciones y Empresas Científicas y Tecnológicas

1702902 CONAHCYT

Article

Introduction

In this work, the use of colloidal systems was proposed for cleaning slogans and insignia after anthropogenic activities on the surfaces of historical buildings. An important part of this research consisted of the capacity of the gelling agents available in the laboratory for the preparation of gels. of the reagents used in cleaning. We sought to define the efficiency of the gels and their performance, in order to reduce costs in conservation processes. At the same time, carry out experimental processes of commercial gelling agents in the compatibility of the thinner, since, according to analyzes carried out, it is the most used solvent in the graffiti removal process, as well as the most economical solvent on the list of solvents. tested in the solubility triangles.

Polymeric solids are especially suitable for forming gels thanks to their long chain structure. The flexibility of these chains makes it possible for them to deform to allow the entry of solvent molecules into their three-dimensional structure.

Gels can be classified into two types, depending on the nature of the connections of the three-dimensional network that constitute them.

Chemical gels: are those in which the network is formed through covalent bonds. This type of bond is very strong and its breakdown leads to degradation of the gel. For this reason, it is said that chemical gels are not reversible with temperature; once the bonds are broken, they cannot be re-formed. This type of bonds gives rise to a gelation process.

Physical gels: present a three-dimensional network formed by joints that are not completely stable, but are associated with a bond ↔ non-bond reaction, which can occur in both directions. Generally, the bonds are of the Van der Waals type, much weaker than covalent bonds.

Box 1
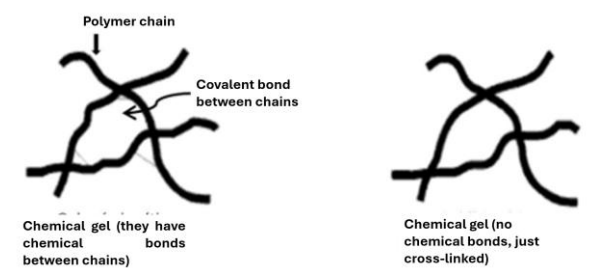
Figure 1

Physical and chemical colloidal systems

With regard to swelling, the essential difference between cross-linked and non-cross-linked polymers is that, in the former, the entry of solvent is not capable of separating the macromolecular chains that form the gel because they are covalently linked, while in the In physical gels the solvation mechanism can unravel and separate from each other as solvent entry into the macromolecular network progresses. This entry reaches a limit or maximum degree of swelling since the covalent structure cannot deform indefinitely. (UNISON, s/f)

A physicochemical system composed of two phases: one continuous, normally fluid, and another dispersed in the form of particles; usually solid, microscopic in size. Gels are semi-solid forms formed by a solvent thickened by the addition of substances of a colloidal nature.

Although the colloid par excellence is one in which the continuous phase is a liquid and the dispersed phase is composed of solid particles, colloids can be found whose components are in other states of aggregation:

Box 2

Table 1

Types of colloids according to the state of their continuous and dispersed phases

		Dispersed phase		
		Gas	Liquid	Solid
Continuous phase	Gas	It is not possible since all gases are soluble in each other.	Liquid aerosol. Example: Fog, mist	Solid aerosol. Example: Smoke, suspended dust
	Liquid	Foam. Example: Shaving foam	Emulsion. Example: Milk, sauce, mayonnaise, blood, hand cream	Colloidal Dispersion. Example: Paints, Chinese ink
	Solid	Colloidal Dispersion. Example: Solid foam, pumice stone, Aerogels	Gel. Example: Gelatin, jelly beans, cheese	Solid sol. Example: Ruby Crystal

The use of gels, packs or dressings implies the use of a supporting material that reduces subsequent mechanical action.
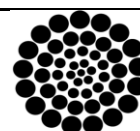
García-Dorado, Samantha, Carranza-Téllez, José, Villegas-Martínez, Rodrigo and García-González, Juan Manuel. [2024]. Solubility study of aerosols and vinyl paint on stone surfaces. Journal of Experimental Systems. 11[30]-1-6: e31130106.
DOI: https://doi.org/10.35429/JOES.2024.11.30.1.6

It allows you to control the amount of the selected cleaning agent and prolong contact times with the wall. Thickeners such as cellulose ethers, agar-agar, carbogel or carbopol are macromolecular substances that, when mixed with organic solvents or water, generate highly viscous solutions. For their part, the supports or supports do not form true gels, but rather pastes or emulsions.

The supports are inert and among the most used is cellulose pulp, it is composed of pure cellulose fibers of different lengths. Among the absorbent clays used, there is sepiolite and attapulgite.

Colloidal or micronized silica also stands out as a support. In addition to the wax that can be used to generate stearic emulsions called pappina, there is Japanese paper that, on many occasions, is also used as an intermediate layer between another support and the work to avoid residues of the second.

Gels are formulations that consist of a solvent or mixture of solvents and a thickener that gels the solution. Thanks to the high viscosity of the system, the penetration of the components into the pictorial layer is limited and controlled, allowing controlled contact for a certain time.

Carbopol produces carboxylate ions (COO-) that can complex certain bivalent and trivalent ions such as calcium or magnesium present in wall paint. If this reaction occurs, Carbopol becomes insoluble in water and can present a clear rinsing problem. It is established that due to this ionic character, it should not be used on surfaces that contain humidity or high pH such as wall paints.

In their study, Carlon and Petersen (2019) carried out artificial aging tests on seven different surfactants. The result is that Ethomeen C12 breaks down over time into small volatile molecules and after 36 hours of artificial aging, no traces or damage to the paint are detected. As for Ethomeen C25, its presence is reduced by 60% during the first 48 hours. Being, together with Agar, the best gelling agent for use in cleaning stone supports.

Pink quarry

The understanding of the intervention processes requires material knowledge of its elements, compounds and the understanding of the physical, chemical and mechanical phenomena that are required for the task, in the case of this series of characterization of materials for the removal of paint from spray graffiti and vinyl paint is based on knowledge of the material you want to clean, pink quarry.

Rocks are divided into three different groups: igneous, sedimentary and metamorphic.

- Igneous Rocks: They are formed by the cooling and crystallization of magma, forming hard and firm rocks. Within igneous rocks there are extrusive and intrusive rocks.

- Extrusive: They are formed when lava cools on the outside of the Earth's mantle or when pyroclastic material is also expelled, such as; glass, ashes and slag consolidate and cool outside.

- Intrusive: They are formed when magma solidifies within the Earth's crust, leaving the rocks buried.

- Sedimentary Rocks: They are formed by the fragmentation or erosion of igneous rocks. The fragmentation of these rocks is known as sediments, these are continuously deposited in a single place where they are compacted and carry out lithification processes, forming sedimentary rocks.

- Metamorphic Rocks: They are formed by the burial of sedimentary rocks in the Earth's crust, being affected by agents of metamorphism, transforming into metamorphic rocks. Extrusive igneous rocks of pyroclastic material form rocks with a microcrystalline texture, which are called tuffs.

The pink volcanic tuff, cantera ignimbrite, is a stone abundant in pumice, quartz and sanidine phenocrysts, it is pinkish in color and is very abundant in the geographical area of San Luis Potosí, Zacatecas, Guanajuato and Morelia.

García-Dorado, Samantha, Carranza-Téllez, José, Villegas-Martínez, Rodrigo and García-González, Juan Manuel. [2024]. Solubility study of aerosols and vinyl paint on stone surfaces. Journal of Experimental Systems. 11[30]-1-6: e31130106.
DOI: https://doi.org/10.35429/JOES.2024.11.30.1.6

The abundance of pink quarry allowed it to be one of the main construction materials, it is present in historical monuments, colonial centers, and in artistic manifestations. However, tuffs are very susceptible to deterioration or alteration of their physical-chemical properties, if are exposed to the elements. Some of the main causes of damage to stone material are strong wind currents, natural light, high temperatures, in conjunction with relative humidity. (Pedroza, 2019)

Moisture, whose presence may be due to rain, condensation or capillary rise, plays a key role in the degradation of porous materials, being directly or indirectly responsible for various decomposition processes, such as freeze-thaw cycles, salts soluble substances, crystallization cycles, biological growth, chemical attack by acid from rain and wind erosion.

Atmospheric movement and humidity have negative effects on conservation. Wind can cause extensive damage to soft rock due to the particles it carries, while changes in temperature and frost can cause fragmentation and splintering in wet environments creating internal stresses. While the polluted atmosphere causes deterioration of the rock in the form of chemical dissolution with the effect of water and organisms (lichens, fungi, bacteria and moss), thin layers of dust that cover the rock generally accumulate and form layers that affect to the entire rock structure.

Background

Molina (2016) studied Intelligent and non-invasive methodologies using nanotechnology for the maintenance, conservation and restoration of heritage buildings. concluded that the treatment of heritage buildings with nanocomposites allows for more efficient maintenance of them and contributes to their conservation.

Morales (2024) evaluated three types of surface coatings applied to quarry stone samples: a coating based on calcium hydroxide, and two commercial coatings based on organosilicon. Surface color of the quarry, water absorption by capillarity and contact angle monitoring were analyzed before, during and after exposure to chemical and natural deterioration.

Di Napoli et al. (2024), carried out a conservative restoration intervention, the structural consolidation and security of the monumental staircase on the Po River side, the restoration of the plaster and the review of the architectural finishes of the castle façade. The methodology chosen based on historical research, physicochemical analyzes of materials and sampling, helped define the most appropriate restoration techniques to guarantee the authenticity and historicity of the monument. The criteria followed were "minimal intervention", "reversibility" and "physicochemical compatibility" of the materials used.

Barrios (2024), presents the contribution of Paolo Marconi by pointing out the importance of recovering the use of traditional techniques and materials in restoration. He left evidence in his books and articles, also in collective works such as the manuali del recupero of Rome and Palermo, which constitute a commitment to recover and transmit the constructive knowledge peculiar to each region or city of Italy.

Methodology

Based on the information collected and the resources delimited by the scope of the conservation laboratory of the INAH Zacatecas center, in relation to the material and equipment, it was determined that:

- The focus of the tests will be based on the elimination of acrylic paint (lacquers) and the elimination of water-soluble vinyl paint, on pink quarry surfaces obtained from pink quarry deposits in the metropolitan area of Guadalupe Zacatecas, samples with diverse physical characteristics.

- The solvents to be used will be determined by the results obtained after solubility calculations using tools such as the Teas solubility triangle, Cemoneci solubility values, as well as the data provided by theoretical values of London dispersion forces, dipole and hydrogen bond.

García-Dorado, Samantha, Carranza-Téllez, José, Villegas-Martínez, Rodrigo and García-González, Juan Manuel. [2024]. Solubility study of aerosols and vinyl paint on stone surfaces. Journal of Experimental Systems. 11[30]-1-6: e31130106.
DOI: https://doi.org/10.35429/JOES.2024.11.30.1.6

– The conservation conditions of the specimens will be equalized in relation to the current deterioration on the stone surfaces, using the use of cleaning techniques observed in graffiti removal processes, using physicochemical cleaning with brushes of different hardness, brushes, swab cleaning.

– Agar and gelatin will be used as a gelling substance for the colloidal systems and the degree of effectiveness in the removal of acrylic paint (lacquers), vinyl paint with different degrees of solubility in water will be verified, the effect of waste generated will be determined. and the degree of penetration into the pores.

The solubility values were determined according to the triangle of firebrands based on the main characteristics of the Alkenyl (ethylene; vinyl) functional groups and the Acryl functional group. The values of permanent dipole force, values of hydrogen bond force, values of Van der Waals forces in the literature.

The spaces were delimited in relation to the real conditions of the stone surfaces of the historic buildings in the city of Zacatecas, testing the colors pink, purple, blue, white, red, of acrylic paint (lacquer) on surfaces where the stone had the porous surface, smooth surface, sanded surface, surface with the presence of salts. At the same time, the areas where the pure vinyl paint would be tested and diluted to 50% of the main colors obtained by the sample, which are green, pink, purple.

In the experimental process, information on the effect of citric acid nanoparticles, colloidal silver, xylol, and citric acid essential oil on test tubes of vinyl paint and acrylic paint (lacquers) was incorporated directly. In order to identify the physical behaviors of the paint when directly exposed to solvents.

Solubility tests were carried out on samples of acrylic paint and vinyl paint, testing the dissolution phenomenon of the solvents characterized in table 3, using as samples the color pink, purple and blue in the acrylic paint (lacquers), and the color green, black, pink and purple in undissolved and 50% vinyl paint.

Prior to the preparation of gels, the behavior of the paints in pure state in the case of vinyl paint and in a 50% solution in water was carried out, and the behavior of acrylic paint (lacquers) in aerosol was studied. Using the thinner as a solution for making gels.

Results

All the solvents established in the theory were tested, of which those that obtained the best results were those that were carried out with the use of benzene and cyclohexanone, since it does not generate migration of the paint, nor the presence of halos on the stone surface.

The use of benzene, although it generates optimal results, the best for this test, has important implications regarding its use due to the damage to health it generates, however, its management requires special conditions found in the standard. STP 014 of Mexican standards. As well as the safety data of the product technical sheet. The effect of the colloidal system for benzene requires special handling due to its poorly soluble characteristics in water, the handling of a gel of a different nature is required, the use of sol gel for the colloidal system is proposed. Or identify the stability of the gel based on gelatin and agar in a solution with a mixture of alcohol in the solvent.

Cyclohexanone has more stable characteristics in terms of pH for agar or gelatin gels, at the same time it presents fewer implications for health risks to human personnel, and it is soluble in water.

Similarly, optimal results were obtained with the use of thinner, with the characteristics that the thinner generates discoloration on the stone surface, generating a whitish mark if applied directly; however, in all cases it was carried out. a reaction and a paint dispersion phenomenon. That is why the results obtained with the colloidal system reduced the discoloration effect on the stone surface, obtaining good results in the removal of vinyl and acrylic paint, since the paint migrates to the plastic film generated by the colloidal system (gel).

García-Dorado, Samantha, Carranza-Téllez, José, Villegas-Martínez, Rodrigo and García-González, Juan Manuel. [2024]. Solubility study of aerosols and vinyl paint on stone surfaces. Journal of Experimental Systems. 11[30]-1-6: e31130106.
DOI: https://doi.org/10.35429/JOES.2024.11.30.1.6

It does not generate a residue, since the plastic film migrates the paint. However, the use of water as a washing effect could generate penetration of dispersed particles inside the pores; the real effect of the absorption phenomenon will be tested by means of stratigraphy in the specimens.

Regarding the effectiveness of the gels, those that presented the best results in dissolving acrylic and vinyl paint were the 20% 30% gelatin gels and the 40% agar gel.

The effect of colloidal silver on the surface of vinyl paint and acrylic paint in the stone material generates inconclusive results regarding its effectiveness in dissolving vinyl and acrylic paint, since a reaction is generated with the surface, it is unknown. this stage of the project if the reaction is generated by the minerals of the stone material or by the functional groups of the acrylic and vinyl paint.

In the case of acid, an effect similar to that of thinner is generated, in the same way the biggest problem lies in the fact that the dissolution of vinyl and acrylic paint generates discoloration of the surface of the stone material. And the problem with the colloidal system is the degree of acids that generates problems for the system.

Conclusions

In relation to the scope established in this work, it is recognized that the result obtained in terms of information is part of a stage that requires the analysis of the behavior of the reactants over time, where their effect is evaluated in real environmental conditions. in order to determine the safety of the processes used in its use as a cleaning methodology for work of this nature.

At the same time, data analysis information is required with specialized equipment that is not available in the area laboratory. The information collected allows us to provide a solution in terms of intervention, since solutions were found for the elimination of graffiti and vinyl paint on volcanic tuff, data that is proven by theoretical information and information, generating optimal safeguard solutions with relation to existing ones carried out by untrained personnel.

It was found that the use of the gels tested with a thinner solution generates benefits over the methods tested so far, since no residue or plastic film is generated that persists on the surface, generating problems of buffering or waterproofing of the stone material, In turn, the search for buffer reagents that do not modify the degree of acidity over time and the search for agents that allow high concentrations of solvent without the expansion of the system inside it are promoted. As an analysis of the phenomenon, it is suggested for intervention to try the dissolution of paint molecules on the surface and the absorption of systems that generate force contrary to the displacement movement on the surface.

References

Basic

Barrios Rozúa, J. M. (2024). Técnicas tradicionales optimizadas en la restauración. La crucial aportación de Paolo Marconi. *Informes De La Construcción*, *76*(573), 6602.

Di Napoli, C., Garis, M., Dameri, A., Soldati, C., & Frugoni, E. (2024). Turín. Castillo de Valentino. Restauración de la escalera monumental y de la fachada lateral del rìo Po. *Mimesis.Jasd*, *4*(3), 39–44.

Molina-Prieto, L. F. (2016). Nanotecnología: herramienta inteligente para la conservación del patrimonio arquitectónico y urbano. *Revista De Investigación*, *9*(1), 7–22.

Morales-Vázquez R. (2024) Estudio comparativo de tres recubrimientos superficiales usados en la conservación del patrimonio arquitectónico de cantera. Consultado: 1 de julio de 2024.

Pedroza Daniel, EVALUACIÓN DE UN MATERIAL COMPUESTO CON MATRIZ POLIMÉRICA Y REFUERZO CERÁMICO, PARA RESTAURACIÓN DE TOBA VOLCÁNICA ROSA". 2019. Facultad del Hábitat C.R.B.C.M.

UNISON. Universidad de Sonora. Geles. s/f. Disponible en: Recuperado el 4 de junio de 2024

Anticorrosive SiO₂-PDMS ceramic coating: effect of viscosity and functional group on the siloxane chain

Recubrimiento cerámico anticorrosivo SiO₂/PDMS: efecto de la viscosidad y grupo funcional en la cadena siloxano

Salazar-Hernández, Carmen*[a], Salazar-Hernández, Mercedes[b], Mendoza-Miranda, Juan Manuel[c] and Elorza-Rodríguez, Enrique[d]

[a] ROR Instituto Politécnico Nacional-UPIIG • D-4418-2019 • 0000-0002-6901-2937 • 105461
[b] ROR Universidad de Guanajuato • LTF-1226-2024 • 0000-0001-8039-8124 • 446271
[c] ROR Instituto Politécnico Nacional-UPIIG • LTF-7054-2024 • 0000-0003-4777-767X • 295057
[d] ROR Universidad de Guanajuato • LTF-1875-2024 • 0000-0001-8633-6063 • 218740

Abstract

Nowadays, a variety of techniques exist for mitigating the effects of corrosion, including the use of anticorrosive coatings. In this study, we investigate the impact of viscosity on the final quality of a silica/PDMS-based ceramic coating, synthesized through sol-gel methodology. The polycondensation of tetraethylorthosilicate (TEOS) with polydimethylsiloxane (PDMS) was conducted at concentrations of 10, 20, and 40 wt.%, employing DBTL as a catalyst. The coatings were deposited on Al-6061 surfaces via immersion. Infrared spectroscopy indicates the integration of the inorganic phase (SiO₂; 1100 cm⁻¹, 720 cm⁻¹) with the siloxane chain (PDMS; 2900 cm⁻¹, 1250 cm⁻¹, 920 cm⁻¹, 785 cm⁻¹). As the siloxane chain length increased, modifications to the silica structure were observed, with the appearance of signals at 889 cm-1, 867 cm-1, and 835 cm-1. Conversely, the gelation times are reduced in proportion to the PDMS content in the sol solution. Therefore, to obtain smooth and homogeneous finishes, different gelation times are required when applying solutions with viscosities between 5 and 12 mPa·s. These coatings exhibited the most significant increase in corrosion resistance, reaching approximately 75%.

Resumen

Actualmente, existen diferentes métodos que mitigan los efectos de la corrosión, entre los cuales se encuentran los recubrimientos anticorrosivos. En este trabajo se reporta el efecto de la viscosidad sobre el acabado de un recubrimiento cerámico de base sílice/PDMS, que se obtiene mediante la metodología sol-gel, llevando a cabo la policondensación del tetraetilortosilicato (TEOS) con polidimetilsiloxano (PDMS) en concentraciones del 10, 20 y 40 % en peso, usando DBTL como catalizador. Los recubrimientos se depositaron sobre superficies de Al–6061 por inmersión. La espectroscopia de infrarrojo indica la integración de la fase inorgánica (SiO2; 1100 cm⁻¹, 720 cm⁻¹) con la cadena siloxánica (PDMS; 2900 cm⁻¹, 1250 cm⁻¹, 920 cm⁻¹, 785 cm⁻¹). Acorde con el incremento de la cadena siloxánica, se observó la modificación en la estructura de la sílice, apareciendo las señales a 889 cm⁻¹, 867 cm⁻¹ y 835 cm⁻¹. Por otra parte, los tiempos de gelificación se reducen en función del contenido de PDMS en la solución sol, por lo que, para obtener acabados libres de grumos y homogéneos, se requieren diferentes tiempos de gelificación al aplicar soluciones con viscosidades entre 5–12 mPa.s. Estos recubrimientos fueron los que mostraron un mayor incremento en la resistencia a la corrosión, de alrededor del 75%.
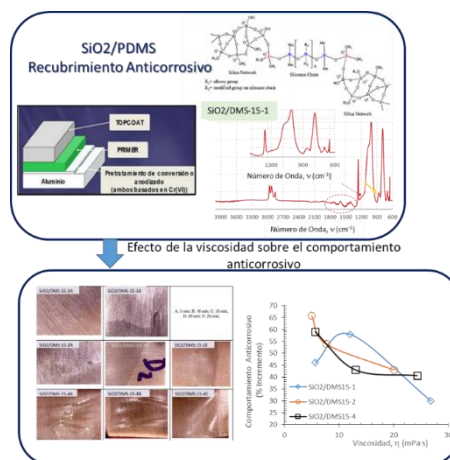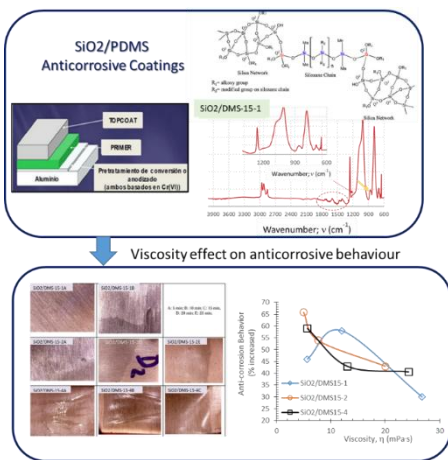
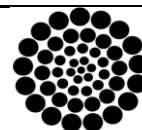SiO₂/PDMS, viscosity, Corrosion mitigating, Infrared spectroscopy, Organic-inorganic coating

SiO₂/PDMS, Viscosidad, Reducción de corrosión, Orgánico-inorgánico cerámico, Espectroscopia de infrarrojo

Journal of Experimental Systems

Article

Introduction

Corrosion is a physicochemical phenomenon that causes the degradation of metals, resulting in the loss of physical properties, such as mechanical strength. In severe cases, corrosion can even lead to the complete degradation of the metal. The phenomenon of corrosion affects all metals and alloys utilized in industrial contexts. Figure 1a illustrates the impact of corrosion on an aircraft comprising an aluminum-silicon alloy (Al-6061) fuselage. In saline and humid conditions, these alloys are susceptible to intergranular corrosion (Figure 1b) (Benavides S, 2009; Zhang X, et. al, 2019). To mitigate the effects of corrosion on this metal, coatings are employed to protect the underlying material. These coatings are composed of an anodizing or anticorrosive layer (chromium and chromate base), a primer (organic phase with traces of chromates), and a topcoat (organic phase) or final finish (Cushman A.S, et. al, 1910; Swgelok 2024).
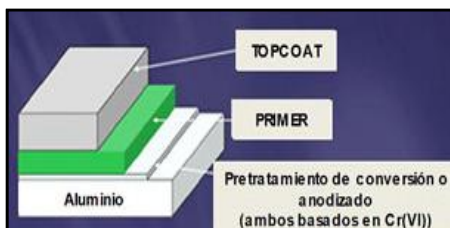
Box 1

(a)
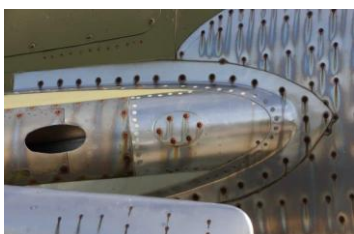
(b)
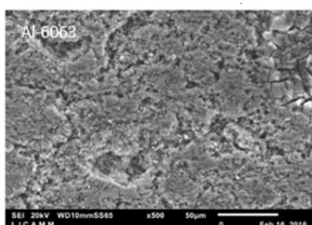
(c)

Figure 1

(a) Corrosion effects in an aircraft (take from https://aerocorner.com/blog/types-of-aircraft-corrosion/) (b) Intergranular corrosion in Al-6061 used in aircraft (take from Salazar-Hernández C, 2017) (c) Composition of a commercial anticorrosion coating (Take from Nace-International http://impact.nace.org/economic-impact.aspx).

At the industrial level, chromium anodizing is a common anti-corrosion agent. This involves the addition of a layer of chromium, which acts as a sacrificial anode. This means that the chromium is corroded by the metal being protected, thereby preventing corrosion. Despite the excellent anticorrosive properties of chromium, it is a toxic element that must be replaced by coatings that are more environmentally friendly (Olorunniwo P.P, 2014; Pellerin C, 2000) Recently, C. Salazar-Hernandez et al. (Salazar-Hernánde C, 2018; Salazar-Hernández C, 2019) have developed hybrid coatings based on silica and polydimethylsiloxane (PDMS). In these coatings, PDMS is cross-linked into the silica network (see Figure 2), which allows the synthesis of coatings with high mechanical stability, good adhesion, and good corrosion resistance on Al-6061. Others, anticorrosive coatings are compounds with organic and organic fragment, where the inorganic network increased the anticorrosive behavior or chemical stability (Ghogde N.R, 2024; Deng Y, 2024; Fu Y, 2022).

Box 2
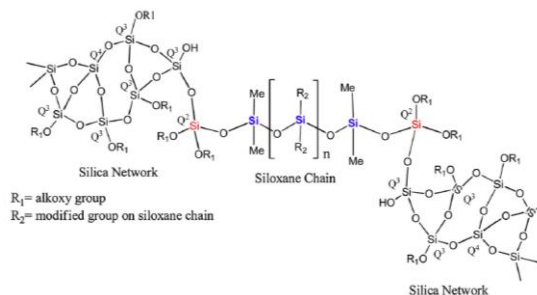
Figure 2.

Chemical structure of SiO_2/PDMS hybrid material
Source: (Salazar-Hernández C, 2019)

Experimental procedure

SiO2/PDMS Ceramic Synthesis

The coatings were obtained via the sol-gel methodology, using tetraethylorthosilicate (TEOS; 99% purity; Fluka) as the starting reagent for silica formation and hydroxylated polydimethylsiloxane (DMS-15; GELEST; 99:12-32 cSt). To this purpose, a sol solution was prepared by mixing the quantities specified in Table 1 and adding 1 wt.% with respect to TEOS of dibutyldilaurate tin (DBTL; 95%, Aldrich), which served as a polycondensation catalyst, thereby facilitating the crosslinking of the silica functional group and the siloxane chains of PDMS.

The sol solutions were heated to 50 °C and maintained at this temperature throughout the experiment. The change in viscosity over time was determined by measuring the viscosity with a Brookfield DV2RLV viscometer, using the UL adapter and controlling the temperature at 50 °C with a TC-650 recirculator.

Box 3		
Table 1		
Quantities used for the synthesis of the sol solution		
	TEOS (g)	DMS-15 (g)
SiO$_2$/DMS-15-1	10	1
SiO$_2$/DMS-15-2	10	2
SiO$_2$/DMS-15-4	10	4

Application of SiO$_2$/PDMS to Al6061 samples

Thin sheets of Al-6061, measuring 3 mm in thickness and 2x3 cm in dimension, were cut. Prior to the application of the coating, the samples were subjected to abrasion with 600-grit sandpaper to remove any residual pollution. Subsequently, the samples were washed twice with distilled water and, finally, once with reagent-grade ethanol, with the objective of drying them in an oven at 50 °C for three hours. The coatings were deposited using the immersion technique, with an immersion speed of 1 mm/min, and were then left to dry at room temperature for 24 hours.

Coating Characterization

Infrared spectroscopy: Infrared spectra were obtained using a Thermo Scientific Nicolet iS10 ATR-FTIR instrument. The average of 32 scans was measured in a spectral window of 4000–600 cm^{-1}, with a resolution of 4 cm^{-1}.

Physical Characterization: Leeb hardness. Leeb hardness was measured using a UNI-T UT-347A instrument according to the recommendations of ASTM A956/A956M-17a.

Adhesion measurement: The force required to achieve peel of the coating was determined using the pull-off test method with a PosiTest AT-A instrument according to ASTM D4541.

Corrosion measurement

An evaluation of corrosion was conducted. Corrosion tests were conducted on a Peak Tech DIT-105 bench with a DCpower-2250 adapter.

In this configuration, the voltage and current generated in the galvanic pile formed by the Al/6061 plate with and without coatings as the anode, and graphite as the cathode, were measured. A 3.5% w/v NaCl solution with a pH of 3 was used, and to acidify, concentrated HCl was added dropwise. A constant current of 0.5 A was applied for 2 h, after which the weight loss generated was subsequently measured and the corrosion rate determined according to Equations 1 and 2 [6, 10, 11].

$$V_c = \frac{\Delta m}{A \cdot t} [=] \frac{kg}{m^2 \cdot s} \qquad (1)$$

$$V_{cp} = \frac{V_c}{\rho} = \left[\frac{mm}{año}\right] \qquad (2)$$

Results

Chemical characterization of SiO$_2$/PDMS ceramics

Figure 3 shows the spectrum corresponding to the SiO$_2$/DMS–15–1 modified ceramic, in which the formation of the silica network from TEOS is identified. The Si–O–Si bond is observed at 1010 cm^{-1} (signal A; intense and wide band) and at 720 cm^{-1} (signal A; low intense band). Furthermore, the integration of the DMS siloxane chain (–Si–O–Si–) is corroborated by the presence of the siloxane bond in the E signal at 920 cm^{-1} (small and broad) and at 785 cm^{-1} (intense and thin), as well as by the band at 1250 cm^{-1}, which identifies the Si-C bond (D signal). In the 2900–2700 cm^{-1} region, the –CH$_3$ groups of DMS–15 and the unreacted –CH$_2$CH$_3$ groups of the alkoxide were identified (signal B). Therefore, it can be concluded that the reaction conditions allow for the formation of crosslinks between the silica network formed by the silicon alkoxide and the siloxane chain fragments of PDMS (Launer P, 2013).

On the other hand; small board signals around the 1100 cm^{-1} was observed indicated the formation of different network silica size. These are remarked with circles and arrows; the different silica clusters are increased according to amount of siloxane chain that was added. Then, major modification in the size of silica network was obtained for ceramic with 40%p of DMS-15 (siloxane chain).

Salazar-Hernández, Carmen, Salazar-Hernández, Mercedes, Mendoza-Miranda, Juan Manuel and Elorza-Rodríguez, Enrique. [2024]. Anticorrosive SiO$_2$-PDMS ceramic coating: effect of viscosity and functional group on the siloxane chain. Journal of Experimental Systems. 11[30]-1-7: e41130107.
DOI: https://doi.org/10.35429/JOES.2024.11.31.4.7

According to infrared results a similarly structure to POSS/PDMS (polyhedral oligomeric silsesquioxane/polydimethylsiloxanr) was observed (Feng X, 2024).

Box 4

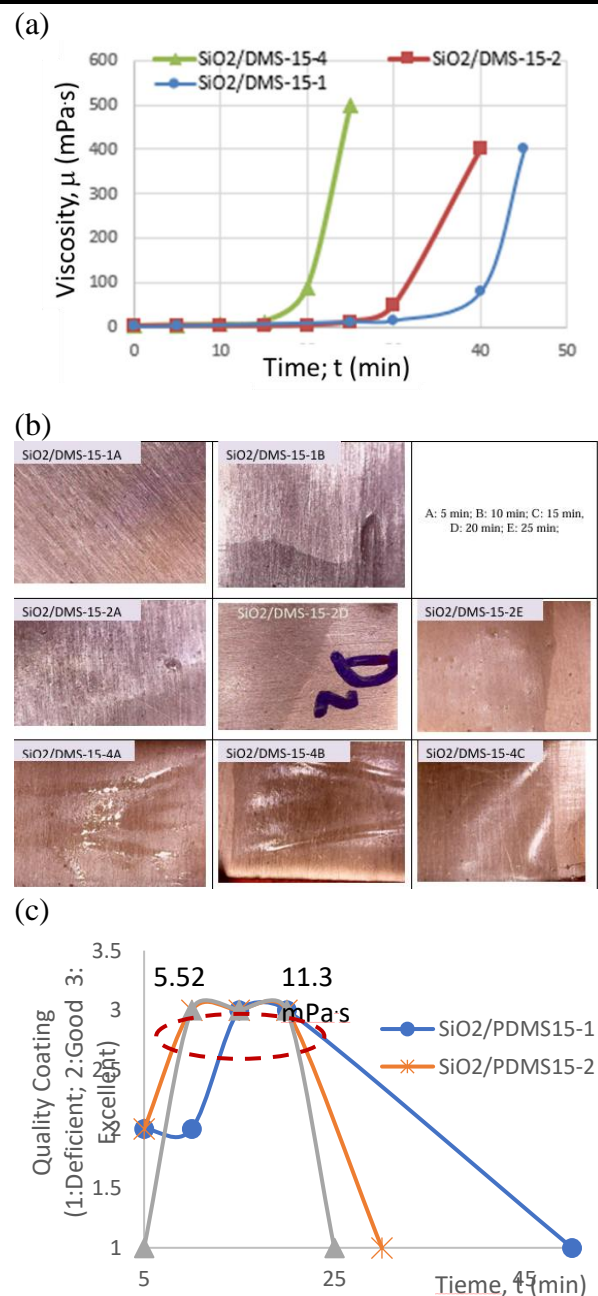a) SiO2/DMS-15-1

b) SiO2/DMS-15-2
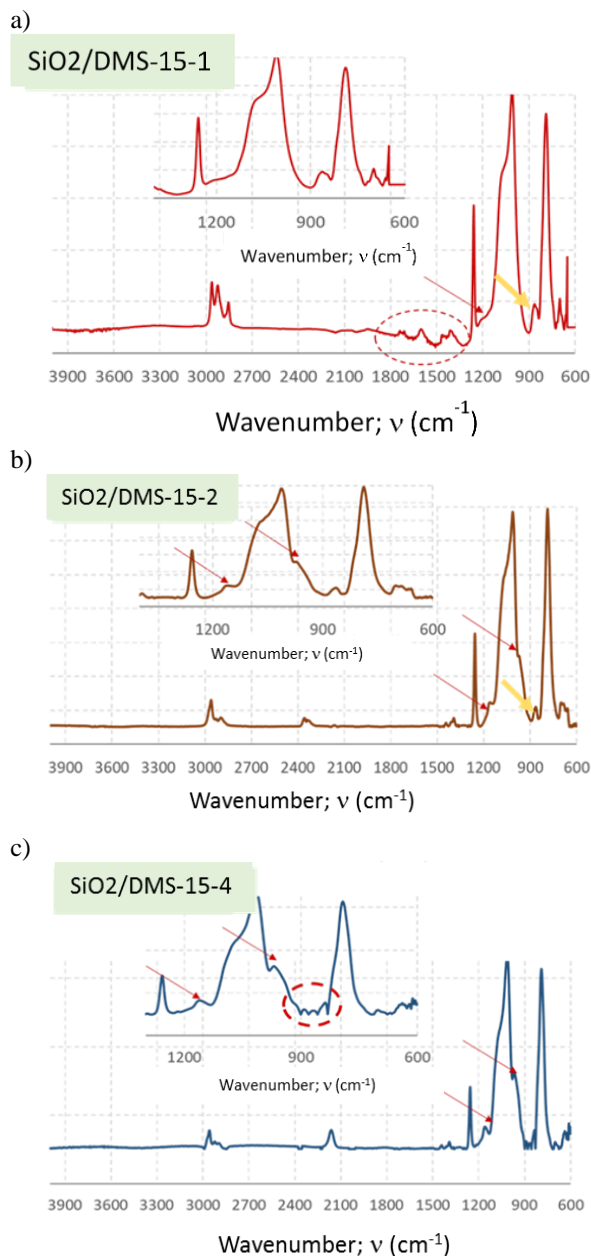
c) SiO2/DMS-15-4

Figure 3

Effect of the siloxane chain in the hybrid ceramic structure (SiO2/DMS-15)

Effect of viscosity on the texture and physical properties of the coating

Figure 4a shows the effect of the siloxane chain on the gel point; where this was modified of 40 min (SiO2/DMS-15-1) to 20 min (SiO2/DMS-15-4) indicating an acceleration in the polycondentation between the silica fragments and the siloxane chain.

On the other hand, the Figure 4b shown the quality coating obtained for different viscosity; in the Figure 4c is indicated the impact of viscosity on the coating finish, as well as the siloxane chain content. At a mixing or gelling time of 10 minutes, the solutions behave as Newtonian fluids with a viscosity of approximately 5 mPa–s, forming thin coatings for concentrations of 10 and 20 wt.% PDMS. As the solid network forms, the viscosity increases, reaching a value of between 10 and 15 mPa–s. after 20 minutes. This results in the formation of thick coatings with clump formation at concentrations of 20 and 40 wt 7%, indicating an enhanced ability to coat the metal surface.
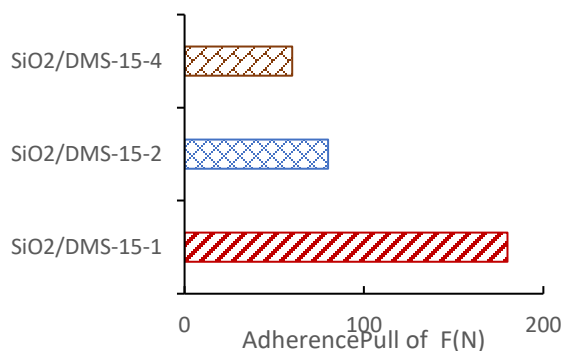
Box 5

Figure 4

(a) Gelling curve for SiO2/DMS-15 ceramics (b) quality coatings obtained to different viscosity (c) effect of the viscosity on quality coatings
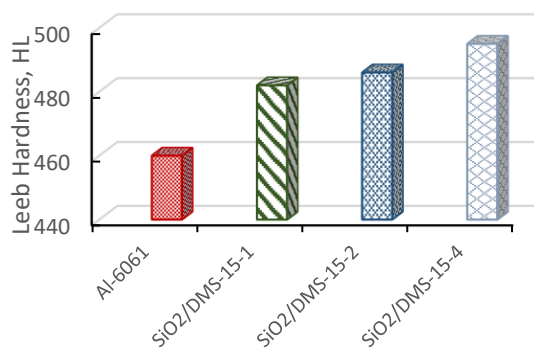
Figure 5a shows the impact of PDMS content in the ceramic lattice on its adhesion. It was observed that as the amount of PDMS decreases the adhesion of the hybrid ceramic with the metal surface increases. In contrast, the hardness (Figure 4b) exhibited an inverse relationship, whereby an increase in hardness was associated with an increase in PDMS content in the ceramic structure. While both properties are crucial, adhesion should be a critical consideration in a coating, as a lack of strong interaction with the metal surface can result in removal and a diminished protective effect.

For the 20 and 40 % concentrations of ceramics, the greatest enhancement in corrosion resistance was observed for a viscosity of approximately 5 mPa–s, which corresponds to a gelation time of between 5 and 10 minutes.

Box 7

Figure 6
Effect of viscosity on corrosion resistance of Al-6061

Box 6

(a)

(b)

Figure 5
Physical properties of coatings with viscosities of 10–15 mPa–s (a) adhesion (b) Leeb hardness

Resistance to corrosion

Figure 6 shows the effect of viscosity on corrosion resistance. It can be observed that the highest corrosion resistance is obtained at a viscosity of approximately 10 mPa–s (10–15 min of gelation) for a PDMS concentration of 10 % in the siloxane chain, as this provides a surface finish that is superior to that of other concentrations.

Conclusions

The viscosity of the sol solution employed to obtain the coatings has an impact on the adherence and hardness of the ceramic deposited on the metal substrate. Deposits formed between 5 and 10 minutes of gelation (approximately 5–12 mPa–s) exhibit enhanced adherence and mechanical stability, as well as a greater degree of homogeneity. These coatings are free of clumps or very thin, and they do not completely cover the roughness of the metal.

Acknowledgements

Statements & Declarations

Consent to participate and Consent for publication

The authors express their approval to participate and publish this work in ECORFAN Journal

Salazar-Hernández, Carmen, Salazar-Hernández, Mercedes, Mendoza-Miranda, Juan Manuel and Elorza-Rodríguez, Enrique. [2024]. Anticorrosive SiO₂-PDMS ceramic coating: effect of viscosity and functional group on the siloxane chain. Journal of Experimental Systems. 11[30]-1-7: e41130107.
DOI: https://doi.org/10.35429/JOES.2024.11.31.4.7

Conflict of interest

The authors declare no interest conflict. They have no known competing financial interests or personal relationships that could have appeared to influence the article reported in this article.

Author contribution

All authors contributed to the development and revision of the manuscript; CSH and MSH (conceptualization, interpretation and analysis date; writing and financial support); EER (interpretation and analysis date and methodology), JMMM (interpretation and acquisitions date). All authors read and approved the final manuscript.

Availability of data and materials

Indicate the availability of the data obtained in this research.

Funding

Abbreviations

SiO_2	Silica ceramic
PDMS	Polydimethylsiloxane
SiO2/PDMS	Silica ceramic modified with polydimethylsiloxane
SiO2/DMS15-1	Silica ceramic modified with 10 % weight polydimethylsiloxane
SiO2/DMS15-2	Silica ceramic modified with 20 % weight polydimethylsiloxane
SiO2/DMS15-4	Silica ceramic modified with 40 % weight polydimethylsiloxane

References

Antecedents

Benavides S, Corrosion in the aerospace industry, in Corrosion Control in the Aerospace Industry, Woodhead Publishing Series in Metal and Surface Engineering, 2009, pp. 1-14. 1

Cushman A.S, Garder H.A, The corrosión and perservation of iron and steel, Mac Graw Hill, New York (1910)

Swagelock, Tipos de Corrosión, Available: Zhang X, Jiao Y, Yu Y, Liu B, Hashimoto T, Liu H, Dong Z (2019) Intergranular corrosion in AA2024-T3 aluminium alloy: The influence of stored energy and prediction, corrosion Science, 155, 1-12.

Basics

Aircraft; Types of aircraft corrosion to be wary of.

Salazar-Hernández C, Salazar-Hernández M, Carrera-Cerritos R, Elorza E, Mendoza-Miranda J.M, Navarro R (2017) DBTL as neutral catalyst on TEOS/PDMS anticorrosive coating, J. Sol-Gel Sci and Technol, 81, 405-412.

Support

International Nace, "Nace International Impact," Olorunniwo O.P; Ige O (2014) Corrosion resistance through the application of anticorrion coatings, In Developments in corrosion protection, M. Aliofkhazraei, Ed., Intech, pp. 242-270.

Pellerin C, Booker S.M (2000) Reflection on hexavalent chromium: health hazards of an industrial heavyweight, Environmetal Health Perspectives, 108 (9), A402-7.

Salazar-Hernández C, Salazar-Hernández M, Carrera-Cerritos R, Mendoza-Miranda J.M, Elorza-Rodríguez E, Miranda-Avilés R, Mocada-Sánchez C.D (2019) Anticorrosive properties of PDMS-Silica coatings: effect of methyl, phenyl and amino groups Progress in Organic Coatings, 136, p. 105220.

Salazar-Hernández C, Salazar-Hernández M, Mendoza-Miranda J.M, Miranda-Avilés R, Elorza-Rodríguez E, Carrera-Cerritos R, Puy-Alquiza M.J (2018) Organic modified silica obtained from DBTL polycondensation catalyst for anticorrosive coating, J. Sol-Gel Sci and Technol, 87 (2) pp. 229-309.

Differerences

Deng Y, Li Z, Yin A, Chen Y, Yang CH, Luo Y, Xe M(2024) A facile method for constructing scalable and low-cost superhydrophobic coating with anti-corrosion and drag-reduction properties, Industrial Crops and Products, 216, 118732.

Dhongde N.R, Adhikari S, Rajaraman P.V (2024) Anticorrosion properties of ionic liquid functionalized graphene oxide epoxy composite coating on the carbon steel for CCUS environment, Preprint. Environmental Science and Pollution Research.

Fu J, Sun Y, Ji Y, Zhang Y (2022) Fabrication of robust ceramic based superhydrophobic coating on aluminum substrate via plasma electrolytic oxidation and chemical vapor deposition methods, Journal of Materials Processing Technology, 306, 117641.

Support

Standard Test Method for Leeb Hardness Testing of Steel products. ASTM-A956/A956M-17a.

Standard TEST Method for Pull-Off Strength of Coatings Using Portable Adhesion Testers. ASTM D4541-22.

Discussion

Feng X, Chen K, Guo X, Sun J, Jian Y, Yan W, Qian S, Xu W, Chen D(2024) Structure-property relationship of polyhedral oligomeric silsesquioxanes/polydimethylsiloxane superhydrophobic coatings for cotton fabrics, Progress in organic coatings, 192, 108476.

Launer P.J (2013) Infrared analysis of organosilicon compounds: spectra structure correlations. In: Arkles B (ed). Silicon Compounds Silanes & Silicones, Gelest Inc: Morrisville, PA.

Optimization of the finite element meshing for the fabrication of a M3x12x0.5 screw, in 3D printing

Optimización del mallado en elemento finito para la fabricación de un tornillo M3x12x0.5, en impresión 3D

González-Sosa, Jesús Vicente*[a], Avila-Soler, Enrique[b] and Zavala-Osorio, Yadira[c]

[a] ROR Universidad Autónoma Metropolitana • 0000-0002-1325-0266 • 166452
[b] ROR Universidad Autónoma Metropolitana • 0000-0001-8980-0925 • 360262
[c] ROR Universidad Autónoma Metropolitana • 0000-0001-5337-6624 • 104843

Abstract

Meshing optimization in the finite element method (FEM) is key to designing mechanical components such as screws. This study focuses on the M3x12x0.5 screw, improving its performance and durability through the appropriate selection of meshing parameters. FEM software was used to analyze its behavior under different loads, comparing it with a 3D printed model. The results showed improvements in the accuracy of predictions about resistance, deformation and stress distribution, allowing the design to be optimized. This highlights the relevance of simulation tools in the development of mechanical components.

Objective¶	Methodology¶	Contribution¶
The objective of this section is the optimization of meshing in the finite element method (FEM) for designing mechanical components such as screws.¶	This study focuses on the M3x12x0.5 screw, improving its performance and durability through the appropriate selection of meshing parameters. FEM software was used to analyze its behavior under different loads, comparing it with a 3D printed model.¶	Las mejoras en la precisión de predicciones sobre resistencia, deformación y distribución de tensiones, permitiendo optimizar el diseño. Esto resalta la relevancia de las herramientas de simulación en el desarrollo de componentes mecánicos.¶ ¶

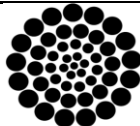**Additive manufacturing, characterization, computational simulation, optimize, identification**

Resumen

La optimización del mallado en el método de elementos finitos (FEM) es clave para diseñar componentes mecánicos como tornillos. Este estudio se centra en el tornillo M3x12x0.5, mejorando su rendimiento y durabilidad mediante la selección adecuada de parámetros de mallado. Se usó software FEM para analizar su comportamiento bajo diferentes cargas, comparándolo con un modelo impreso en 3D. Los resultados mostraron mejoras en la precisión de predicciones sobre resistencia, deformación y distribución de tensiones, permitiendo optimizar el diseño. Esto resalta la relevancia de las herramientas de simulación en el desarrollo de componentes mecánicos.

Objetivo¶	Metodología¶	Contribución¶
El objetivo de este apartado es la optimización del mallado en el método de elementos finitos (FEM) para diseñar componentes mecánicos como tornillos¶	Este estudio se centra en el tornillo M3x12x0.5, mejorando su rendimiento y durabilidad mediante la selección adecuada de parámetros de mallado. Se usó software FEM para analizar su comportamiento bajo diferentes cargas, comparándolo con un modelo impreso en 3D.¶	Las mejoras en la precisión de predicciones sobre resistencia, deformación y distribución de tensiones, permitiendo optimizar el diseño. Esto resalta la relevancia de las herramientas de simulación en el desarrollo de componentes mecánicos.¶

Manufactura aditiva, caracterización, simulación computacional, optimización, identificación

Introduction

Currently, the use of computational tools for product validation has found room for improvement in the development, research and manufacture of specimens for their study with scientific foundations in engineering. In this regard, the Universidad Autónoma Metropolitana, Unidad Azcapotzalco, together with researchers in various engineering areas, have applied techniques such as the Finite Element Method (FEM) and additive manufacturing with 3D printing (MAI3D) to validate industrial case studies. This paper analyzes and establishes the optimization of a screw in order to improve its manufacturing and to understand the physical phenomena involved in the aforementioned specimen.

(Zhu et al. 2023) presents a highly relevant study that highlights how FEM simulators have the right conditions to make a significant contribution to science and technology. This approach takes into account the design considerations and specific parameters of each case study, allowing a better understanding of the physical phenomena affecting the specimens under analysis. In their work, specific conditions related to the case study are presented in order to facilitate the understanding and analysis of the variables involved in the performance of the screw.

Stress concentration in a FEM simulation (Figueroa-Díaz et al., 2019) allows validation of analytical results that would otherwise not be evident in the physical phenomenon. In this sense, simulations offer a valuable alternative to carry out specific studies to improve design conditions and material selection, thus facilitating the feasibility of the characterization methodology.

According to (Lee et al. (2017), simulation behaviors using the FEM are customized, which allows this tool to be efficiently adapted to each case study. This results in significant savings in execution times during the evaluation of such cases. In particular, the importance of torque is highlighted in the corresponding simulation, where a match is obtained in the analysis of a test specimen, which facilitates the identification of improvements.

The current approach (Sheng et.al, 2019) could serve as a guide to select internal fixation parameters in a more efficient manner, potentially facilitating modification and optimization of the internal fixation system. In comparison, a study using a finite element simulator (FEM) of a fastener allows a detailed analysis of the mechanical behavior and factors affecting the performance of the fastening system. This suggests that the integration of both approaches, the present method and the results obtained through FEM simulations, could result in an even more informed and accurate choice of fasteners, thus promoting significant improvements in the design and functionality of the internal fastening system.

(Hsia et al., 2016) emphasize the importance of choosing the right combination of the model in CAD to achieve accurate simulation using the evaluation variables. This choice allows to keep errors to a minimum during the process with the FEM. In this way, evaluation alternatives can be identified, which are carried out in this work under controlled conditions.

According to (Cetin et al., 2022), nowadays, most engineering applications use FEM simulation processes instead of laboratory experiments. This is due to the convenience of running simulations, which have proven to be accurate compared to the results obtained through experimentation.

According to studies by (Chandra et al., 2021), as the simulation load on threaded fasteners increases using FEM, the deformation increases continuously and linearly. It is observed that the load remains within the elastic or plastic zone, without reaching a fracture. Therefore, it is essential to perform mechanical tests to accurately identify this behavior, since the FEM only provides virtual alternatives.

In their study, (Xue et al., 2022) analyzed the optimal fastening of screws used in the medical sector using the FEM. In addition, they examined fracturing through the variables provided by this tool in the context of simulation.

González-Sosa, Jesús Vicente, Avila-Soler, Enrique and Zavala-Osorio, Yadira. [2024]. Optimization of the finite element meshing for the fabrication of a M3x12x0.5 screw, in 3D printing. Journal of Experimental Systems. 11[30]-1-14: e51130114.
https://doi.org/10.35429/JOES.2024.11.30.1.14

The use of simulators, such as the FEM, for the evaluation of mechanical elements enriches technological development and fosters innovation in the engineering field. Several researchers have identified this tool as a valuable resource for improving conditions in the case studies analyzed. The following paragraphs detail the methodology used to simulate the screw in the context of the case study, in order to obtain data to be presented in the results.

Methodology

The procedure to develop this work is given from first making the specimen with a CAD modeler, establishing the dimensions of the screw as a case study, then apply FEM to validate the results, depending on the specific variables in a screw when subjected to torque, accumulate the data, apply optimization steps in the meshing to reach the specimen that meets the mechanical stresses and finally set the parameters for the manufacture of the screw with 3D printing (I3D).

The following paragraphs describe each of the stages mentioned to identify the process in the evaluation of the case study, screw M3x12x0.5.

Specimen modeling: in this section the measurements corresponding to the case study, M3x12x0.5 bolt, are taken into consideration and the dimensional drawing is developed, then the software tools are used to obtain the product in 3 dimensions (solid). Figure 1 shows the general outline of the screw.

Box 1

Figure 1

Sketch of specimen, screw

Source: Own elaboration

According to the conditions of the specimen, screw, shown in Figure 1, it will be analyzed from the mechanical point of view with the torsion parameters and identify the maximum loads it will withstand when manufactured with specific and general I3D materials. Figure 2 shows the drawing of the specimen generated with the CAD software, with the screw specifications.

Box 2
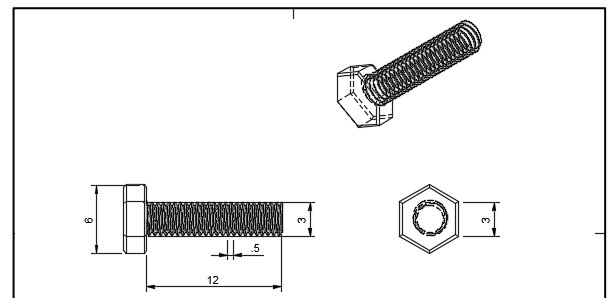
Figure 2

Plan corresponding to the screw to be evaluated

Source: Own elaboration

Figure 3 shows the 3-dimensional model with the parameters and variables defined by the data sheet in the screw classification.

Box 3

Figure 3

Screw M3x12x0.5 elaborated in CAD software

Source: Own elaboration

Figure 3 shows the screw in its three-dimensional perspective to be evaluated with the FEM tool and to obtain the best conditions for its manufacturing with MAI3D.

The materials to be used in the FEM simulations and fabrication in I3D are: Acrylonitrile Butadiene Styrene (ABS), Polylactic Acid (PLA) and NYLON 6/6, for which we have the physical properties identified in Table 1.

González-Sosa, Jesús Vicente, Avila-Soler, Enrique and Zavala-Osorio, Yadira. [2024]. Optimization of the finite element meshing for the fabrication of a M3x12x0.5 screw, in 3D printing. Journal of Experimental Systems. 11[30]-1-14: e51130114. https://doi.org/10.35429/JOES.2024.11.30.1.14

Journal of Experimental Systems

Article

Box 4

Table 1

Physical properties of materials

Material	Property	Value/unit
ABS	Tensile stress	30.46 [MPa]
	Deformation	4.52 [%]
	Hardness	69.2 Shore D
	Flexural modulus	1.08 [GPa]
PLA	Tensile stress	47.95 [MPa]
	Deformation	3.8 [%]
	Hardness	79.8 Shore D
	Flexural modulus	1. 47 [GPa]
NYLON	Tensile stress	33.22 [MPa]
	Deformation	9.17 [%]
	Hardness	62 Shore D
	Flexural modulus	0.78 [GPa]

Source: https://www.matweb.com/index.aspx

The variables analyzed in the FEM software are Flexural Modulus (MF), Deformation (DF) and Stress (EF), which determine the optimal conditions of the specimen for its fabrication in I3D.

FEM application: for the FEM simulation, the parameters shown in Table 2 were considered, which are fundamental for the proper development of the simulations corresponding to the described screw.

Box 5

Table 2

Parameters to be used in the simulation with FEM

Parameter	Description
Material to simulate	Plastic ABS Nylon 6/6 Softe plastic (PLA)
Load	Torque of 1600 Nmm on the screw chord.
Meshing	Parabolic 60° Minimum element size 20%

Source: Own elaboration

The materials designated in the simulation have been chosen because of their use for the manufacture of logs in I3D. After these simulations, some others can be selected from the software databases to achieve the simulation and an approach with the functional materials in the manufacturing process with additive manufacturing.

Regarding the load used in the simulation and shown in Table 2, it has been considered from the technical specifications of bolts made of plastic materials. The load application zone, torsion, is carried out on the rope, which is the weak one of a screw of these characteristics, as far as its size is concerned.

In the case of meshing, it is carried out with the characteristics mentioned in Table 2, which offers a simulation and depending on the results, this parameter will have considerable variations to achieve the optimization of the screw and the correct manufacturing of the specimen. Figure 4 below shows the first simulation for the specimen with the ABS material.
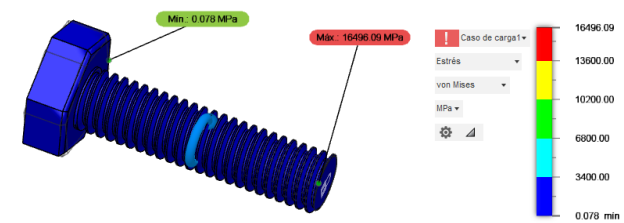
.

Box 6

Figure 4

FEM ABS simulation

Source: Own elaboration

Figure 4 identifies the maximum and minimum value of the Von Mises load in MPa for the specimen with the material called ABS, these values are: minimum 0.078 and maximum 16496, both in MPa. It is observed, according to the color range, that the specimen has no risk of suffering any damage when the corresponding load of 1600 Nmm is applied.

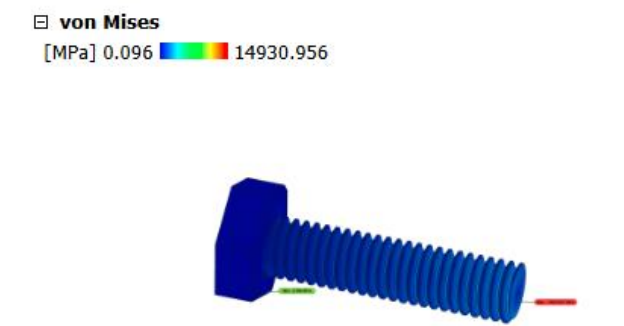Figure 5 below shows the maximum and minimum values for the nylon 6/6 material.

González-Sosa, Jesús Vicente, Avila-Soler, Enrique and Zavala-Osorio, Yadira. [2024]. Optimization of the finite element meshing for the fabrication of a M3x12x0.5 screw, in 3D printing. Journal of Experimental Systems. 11[30]-1-14: e51130114. https://doi.org/10.35429/JOES.2024.11.30.1.14

Box 7

□ von Mises
[MPa] 0.096 ▭ 14930.956

Figure 5
FEM nylon 6/6 simulation

Source: Own elaboration

For the case of the material known as Nylon 6/6, the stress is in the range of 0.096 to 14930.56 MPa, which has a decrease of 9.48% with respect to the ABS material. It is important to mention that in all the simulations the application of the load, torsion, is performed in the same environment, rope, so that the results obtained can be compared and subsequently the corresponding optimization can be carried out. Figure 6 shows the simulation of the third PLA material, which has the qualitative characteristics of being soft.

Box 8

□ von Mises
[MPa] 0.081 ▭ 16402.869
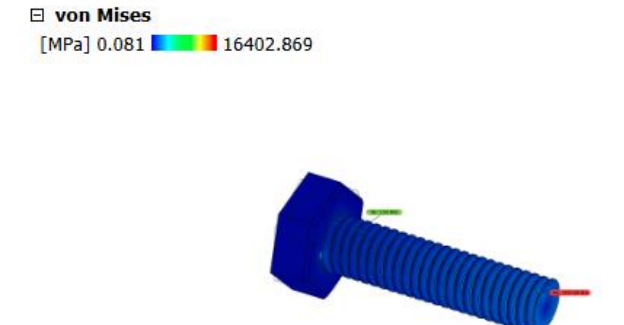
Figure 6
FEM PLA simulation

Source: Own elaboration

Figure 6 shows that the material called soft plastic has the intermediate values among the three cases, 0.081 to 16402.87 MPa, indicating that it is a material that maintains its properties congruent with the other materials.

The three materials have similar behaviors at the time of performing the FEM simulations, however, the following tables will identify the critical aspects of the simulation to identify as far as possible the application of the optimization process.

Table 3 concentrates the data obtained from the FEM simulation for the M3x12x0.5 screw, using the ABS material.

Box 9

Table 3
Simulation data obtained for the screw in ABS material

Material	Property	Value/unit
	Von Mises Stress	16496.09 [MPa]
	Principal Stress	11550.06 [MPa]
	Normal in XX	1663.35 [MPa]
	Normal in YY	2752.77 [MPa]
	Normal in ZZ	4070.01 [MPa]
	To XY cut	2661.74 [MPa]
	To YZ cut	1635.49 [MPa]
	To ZX cut	2523.50 [MPa]
ABS	Total displacement	10.86 [mm]
	X displacement	0.15 [mm]
	Y displacement	10.77 [mm]
	Z displacement	8.41 [mm]
	Total reaction force	31.19 [N]
	Force at X	1.96 [N]
	Force at Y	11.70 [N]
	Force at Z	29.48 [N]
	Deformation	13.28 [%]

Source: Authors.

The values shown in Table 3 are representative in the FEM simulation for the M3x12x0.5 bolt, which has the characteristic of withstanding a force of 31.19 N, when a torque value of 16000 Nmm is applied. This force has a variation of 0.12 to 7% with the materials selected for the screw analysis.

A characteristic for the displacement at the time of performing the FEM simulation is shown in Figure 7, for the ABS material, identifying within the range of colors that it is found with a value of 10.26 mm in the part called the head of the screw, in future simulations it is sought to reduce the value obtained.
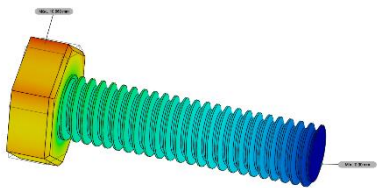
González-Sosa, Jesús Vicente, Avila-Soler, Enrique and Zavala-Osorio, Yadira. [2024]. Optimization of the finite element meshing for the fabrication of a M3x12x0.5 screw, in 3D printing. Journal of Experimental Systems. 11[30]-1-14: e51130114.
https://doi.org/10.35429/JOES.2024.11.30.1.14

Box 10

Figure 7

Displacement in the ABS material specimen

Source: Own elaboration

Table 4 below shows the simulation values applied to the screw with Nylon 6/6 material, highlighting the representative physical properties.

Box 11

Table 4

Simulation data obtained for the screw in Nylon 6/6 material

Material	Property	Value/Unit
	Von Mises Stress	14930.96 [MPa]
	Principal Stress	4612.21 [MPa]
	Normal in XX	970.58 [MPa]
	Normal in YY	2919.58 [MPa]
	Normal in ZZ	2172.08 [MPa]
	To XY cut	7059.78 [MPa]
	To YZ cut	2544.79 [MPa]
	To ZX cut	3081.28 [MPa]
Nylon 6/6	Total displacement	16.41 [mm]
	X displacement	2.64 [mm]
	Y displacement	2.57 [mm]
	Z displacement	0.72 [mm]
	Total reaction force	33.54 [N]
	Force at X	11.51 [N]
	Force at Y	10.46 [N]
	Force at Z	20.75 [N]
	Deformation	8.63 [%]

Source: Own elaboration

The percentage of comparison with respect to the ABS and Nylon 6/6 material, in the main stress property, observed in Table 4, is 60.06%, values that exceed an equilibrium in this parameter.

As in the case analyzed with the ABS material, now in Nylon 6/6, Figure 8 shows the color scale for the displacement property.

Box 12
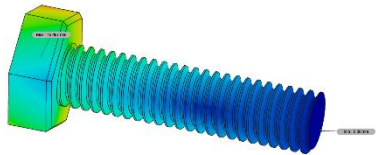
Figure 8

Displacement for Nylon 6/6 material

Source: Own elaboration

The value of the displacement is 16.41 mm, Figure 8, identifying an increase with respect to the previous material. In subsequent simulations we will analyze how to homogenize the property and thus achieve the appropriate optimization for the specimen.

Table 5 shows the effects of the FEM simulation on the PLA material under the stresses applied to each of the simulations with the described variables.

Box 13

Table 5

Data obtained from simulation for the screw in PLA material

Material	Property	Value/Unit
	Von Mises Stress	16402.87 [MPa]
	Principal Stress	11598.67 [MPa]
	Normal in XX	1763.12 [MPa]
	Normal in YY	2856.72 [MPa]
	Normal in ZZ	4166.84 [MPa]
	To XY cut	2633.45 [MPa]
	To YZ cut	1640.10 [MPa]
	To ZX cut	2511.43 [MPa]
PLA	Total displacement	26.92 [mm]
	X displacement	0.367 [mm]
	Y displacement	26.70 [mm]
	Z displacement	20.86 [mm]
	Total reaction force	31.23 [N]
	Force at X	2.06 [N]
	Force at Y	11.70 [N]
	Force at Z	29.46 [N]
	Deformation	32.83 [%]

Source: Own elaboration

For the case of deformation, according to the application of the 16000 Nmm, PLA material, named as soft material, has a higher percentage of deformation compared to ABS and Nylon 6/6, which has the value of 32.83.

González-Sosa, Jesús Vicente, Avila-Soler, Enrique and Zavala-Osorio, Yadira. [2024]. Optimization of the finite element meshing for the fabrication of a M3x12x0.5 screw, in 3D printing. Journal of Experimental Systems. 11[30]-1-14: e51130114.
https://doi.org/10.35429/JOES.2024.11.30.1.14

Figure 9, shown below has the characteristic of observing the displacement, whose zone of action is seen in the upper part of the screw, head, where the applied torque exerts the physical effects for deformation.
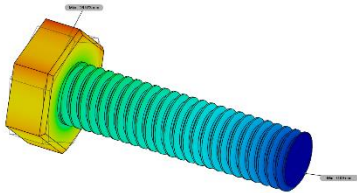
Box 14

Figure 9

Displacement for PLA material

Source: Own elaboration

Each of the figures shown has the characteristic of showing the range of colors that allows to visualize the effect of the load applied during the FEM simulation on the M3x12x0.5 bolt as part of the specimen of study and analysis.

In the following section, part of the data obtained in the optimization of the screw with FEM simulation is described and observed.

Optimization of FEM in the specimen: the optimization part of the screw for its fabrication with I3D will be described in different stages, which are developed below.

First stage: decrease the number of nodes and elements obtained when performing the FEM simulation. In the data of the standard simulations the number of nodes are 16959 and elements 16167, after making the first changes in the simulation 2426 nodes and 9631 elements were obtained, for the following changes 2554 nodes, 10137 elements and in the last change of parameters 5463 nodes with 24257 elements were obtained, which is indicating that simulations 2 and 3 are the ones that decrease these two variables in the meshing for the FEM simulations. Second stage: a change is made in the format for the meshing in the screw, initially we worked with the mesh in parabolic form and the change, to optimize, was carried out with the meshing in linear form. With this variation, the data shown in Table 6 for ABS, Table 7 with Nylon and Table 8 with PLA material are obtained.

Box 15

Table 6

Simulation data obtained for the screw in ABS material optimizing the linear meshing arrangement

Material	Property	Value/Unit
PLA	Von Mises Stress	3713.26 [MPa]
Linear	Principal Stress	1689.89 [MPa]
Meshing	Normal in XX	522.56 [MPa]
	Normal in YY	818.13 [MPa]
	Normal in ZZ	634.43 [MPa]
	To XY cut	1212.17 [MPa]
	To YZ cut	460.17 [MPa]
	To ZX cut	651.38 [MPa]
	Total displacement	9.17 [mm]
	X displacement	0.13 [mm]
	Y displacement	8.89 [mm]
	Z displacement	6.88 [mm]
	Total reaction force	69.78 [N]
	Force at X	6.41 [N]
	Force at Y	35.35 [N]
	Force at Z	59.27 [N]
	Deformation	2.71 [%]

Source: Own elaboration

The use of tables to analyze the improvement in the evaluation parameters highlights the relevance of the simulator in this case study.

Box 16

Table 7

Simulation data obtained for the screw in Nylon 6/6 material optimizing the linear meshing arrangement.

Material	Property	Value/Unit
PLA	Von Mises Stress	3772.34 [MPa]
Linear	Principal Stress	1668.72 [MPa]
Meshing	Normal in XX	401.96 [MPa]
	Normal in YY	827.58 [MPa]
	Normal in ZZ	631.60 [MPa]
	To XY cut	1262.75 [MPa]
	To YZ cut	464.33
	To ZX cut	[MPa]
	Total displacement	691.53
	X displacement	[MPa]
	Y displacement	6.93 [mm]
	Z displacement	0.10 [mm]
	Total reaction force	6.71 [mm]
	Force at X	5.19 [mm]
	Force at Y	70.03 [N]
	Force at Z	5.38 [N]
	Deformation	34.52 [N]
		57.64 [N]
		2.07 [%]

Source: Authors.

Each of the materials evaluated offers characteristics that give value to the FEM analysis.

González-Sosa, Jesús Vicente, Avila-Soler, Enrique and Zavala-Osorio, Yadira. [2024]. Optimization of the finite element meshing for the fabrication of a M3x12x0.5 screw, in 3D printing. Journal of Experimental Systems. 11[30]-1-14: e51130114. https://doi.org/10.35429/JOES.2024.11.30.1.14

Box 17

Table 8

Simulation data obtained for the screw in PLA material optimizing the linear arrangement of the mesh

Material	Property	Value/Unit
	Von Mises Stress	3683.70 [MPa]
	Principal Stress	1705.85 [MPa]
	Normal in XX	584.63 [MPa]
	Normal in YY	812.35 [MPa]
	Normal in ZZ	642.24 [MPa]
	To XY cut	1187.95 [MPa]
	To YZ cut	457.87 [MPa]
PLA	To ZX cut	631.95 [MPa]
Linear	Total displacement	22.65 [mm]
Meshing	X displacement	0.33 [mm]
	Y displacement	21.94 [mm]
	Z displacement	16.97 [mm]
	Total reaction force	69.64 [N]
	Force at X	6.93 [N]
	Force at Y	35.81 [N]
	Force at Z	60.18 [N]
	Deformation	6.66 [%]

Source: Own elaboration

Third stage: the variables to be modified and generate another optimization is the minimum size of elements at 10% with linear arrangement in the mesh, the data are shown in table 9 ABS material, table 10 nylon material and table 11 PLA material, each table with the corresponding physical properties.

Box 18

Table 9

Simulation data obtained for the screw in ABS material by optimizing the size of elements in the mesh

Material	Property	Value/Unit
ABS	Von Mises Stress	3942.40 [MPa]
Minimum	Principal Stress	2048.54 [MPa]
element	Normal in XX	160.28 [MPa]
size at	Normal in YY	764.14 [MPa]
10%	Normal in ZZ	874.34 [MPa]
Linear	To XY cut	1147.46 [MPa]
meshing	To YZ cut	420.68 [MPa]
	To ZX cut	725.29 [MPa]
	Total displacement	9.12 [mm]
	X displacement	0.12 [mm]
	Y displacement	8.79 [mm]
	Z displacement	6.82 [mm]
	Total reaction force	83.49 [N]
	Force at X	7.50 [N]
	Force at Y	26.64 [N]
	Force at Z	49.95 [N]
	Deformation	2.92 [%]

Source: Own elaboration

In this phase, modifications have been taken into account to re-evaluate each of the materials, applying the corresponding loads, in order to identify significant improvements in simulations of this type.

Box 19

Table 10

Simulation data obtained for the screw in Nylon 6/6 material by optimizing the size of elements in the mesh

Material	Property	Value/Unit
Nylon 6/6	Von Mises Stress	4040.32 [MPa]
Minimum	Principal Stress	2047.39 [MPa]
element	Normal in XX	109.25 [MPa]
size at	Normal in YY	774.61 [MPa]
10%	Normal in ZZ	865.84 [MPa]
Linear	To XY cut	1176.75 [MPa]
meshing	To YZ cut	425.70 [MPa]
	To ZX cut	737.10 [MPa]
	Total displacement	6.89 [mm]
	X displacement	0.09 [mm]
	Y displacement	6.64 [mm]
	Z displacement	5.14 [mm]
	Total reaction force	82.58 [N]
	Force at X	6.58 [N]
	Force at Y	26.66 [N]
	Force at Z	49.34 [N]
	Deformation	2.25 [%]

Source: Own elaboration

Box 20

Table 11

Data obtained from simulation for the screw in PLA material by optimizing the size of elements in the mesh

Material	Property	Value/Unit
PLA	Von Mises Stress	3893.97 [MPa]
Minimum	Principal Stress	2048.14 [Mpa]
element	Normal in XX	188.19 [Mpa]
size at	Normal in YY	758.15 [Mpa]
10%	Normal in ZZ	877.32 [Mpa]
Linear	To XY cut	1133.08 [Mpa]
meshing	To YZ cut	418.07 [Mpa]
	To ZX cut	719.44 [Mpa]
	Total displacement	22.52 [mm]
	X displacement	0.29 [mm]
	Y displacement	21.70 [mm]
	Z displacement	16.84 [mm]
	Total reaction force	83.98 [N]
	Force at X	7.98 [N]
	Force at Y	26.64 [N]
	Force at Z	50.32 [N]
	Deformation	7.14 [%]

Source: Own elaboration

González-Sosa, Jesús Vicente, Avila-Soler, Enrique and Zavala-Osorio, Yadira. [2024]. Optimization of the finite element meshing for the fabrication of a M3x12x0.5 screw, in 3D printing. Journal of Experimental Systems. 11[30]-1-14: e51130114.
https://doi.org/10.35429/JOES.2024.11.30.1.14

Fourth stage: modify the angle of rotation in the mesh to optimize the test specimens and compare them with the other FEM simulations obtained. For this purpose, the data are shown in tables 12, 13 and 14, with the same materials as in the previous stages.

Box 21

Table 12

Simulation data obtained for 30° angle in ABS material by optimizing the size of elements in the mesh.

Material	Property	Value/Unit
ABS Pivoting angle 30° Linear meshing	Von Mises Stress	2421.23 [MPa]
	Principal Stress	1436.17 [MPa]
	Normal in XX	129.15 [MPa]
	Normal in YY	607.76 [MPa]
	Normal in ZZ	865.55 [MPa]
	To XY cut	1103.79 [MPa]
	To YZ cut	106.02 [MPa]
	To ZX cut	645.79 [MPa]
	Total displacement	9.03 [mm]
	X displacement	0.05 [mm]
	Y displacement	8.83 [mm]
	Z displacement	7.11 [mm]
	Total reaction force	80.56 [N]
	Force at X	3.85 [N]
	Force at Y	24.47 [N]
	Force at Z	56.96 [N]
	Deformation	1.88 [%]

Source: Own elaboration

As a result of adjusting the parameters in the case study simulations, new opportunities in the field of applied engineering are investigated and evaluated, using screws as a case of analysis.

Box 22

Table 13

Simulation data obtained for 30° angle in Nylon material by optimizing the size of elements in the mesh.

Material	Property	Value/Unit
Nylon 6/6 Pivoting angle 30° Linear meshing	Von Mises Stress	2458.48 [MPa]
	Principal Stress	1429.20 [MPa]
	Normal in XX	107.61 [MPa]
	Normal in YY	564.98 [MPa]
	Normal in ZZ	864.68 [MPa]
	To XY cut	1122.10 [MPa]
	To YZ cut	410.53 [MPa]
	To ZX cut	651.34 [MPa]
	Total displacement	6.78 [mm]
	X displacement	0.04 [mm]
	Y displacement	6.63 [mm]
	Z displacement	5.34 [mm]
	Total reaction force	80.62 [N]
	Force at X	3.20 [N]
	Force at Y	24.43 [N]
	Force at Z	55.72 [N]
	Deformation	1.43 [%]

Source: Own elaboration

Some data may be synthesized to facilitate a statistical analysis in the results section, which provides additional support for enriching studies using simulators such as the one used in this work, which is FEM.

Box 23

Table 14

Simulation data obtained for 30° angle in PLA material by optimizing the size of elements in the mesh.

Material	Property	Value/Unit
PLA Pivoting angle 30° Linear meshing	Von Mises Stress	2402.74 [MPa]
	Principal Stress	1440.10 [MPa]
	Normal in XX	146.51 [MPa]
	Normal in YY	629.53 [MPa]
	Normal in ZZ	867.14 [MPa]
	To XY cut	1094.74 [MPa]
	To YZ cut	403.51 [MPa]
	To ZX cut	642.91 [MPa]
	Total displacement	22.36 [mm]
	X displacement	0.13 [mm]
	Y displacement	21.86 [mm]
	Z displacement	17.60 [mm]
	Total reaction force	80.53 [N]
	Force at X	4.19 [N]
	Force at Y	24.89 [N]
	Force at Z	57.62 [N]
	Deformation	4.64 [%]

Source: Own elaboration

The next section will employ a statistical tool using graphs to support screw production optimization in collaboration with the FEM.

Results

The scatter plots corresponding to some of the data obtained from the tables showing the results of the FEM simulations are presented. Table 15 contains the data to be used to graphically represent the results when performing the simulation on the screw using FEM.

Box 24

Table 15

Representative values for the graphs

Material	EVM [MPa]	DZ [mm]	FR [N]	DF [%]
ABS	16496.1	10.86	31.19	13.28
	3713.3	9.17	69.78	2.71
	3942.4	9.12	83.49	2.92
	2421.2	9.03	80.56	1.88
Nylon 6/6	14931.0	16.41	33.54	8.63
	3772.3	6.93	70.03	2.07
	4040.3	6.89	82.58	2.25
	2458.5	6.78	80.62	1.43
PLA	16402.9	26.92	31.23	32.83
	3683.7	22.65	69.64	6.66
	3894.0	22.52	83.98	7.14
	2402.7	22.36	80.53	4.64

Source: Own elaboration

González-Sosa, Jesús Vicente, Avila-Soler, Enrique and Zavala-Osorio, Yadira. [2024]. Optimization of the finite element meshing for the fabrication of a M3x12x0.5 screw, in 3D printing. Journal of Experimental Systems. 11[30]-1-14: e51130114. https://doi.org/10.35429/JOES.2024.11.30.1.14

Article

The following Figure 10 shows the dispersion of the measurements for each material, as well as the variations in certain parameters.

Box 25
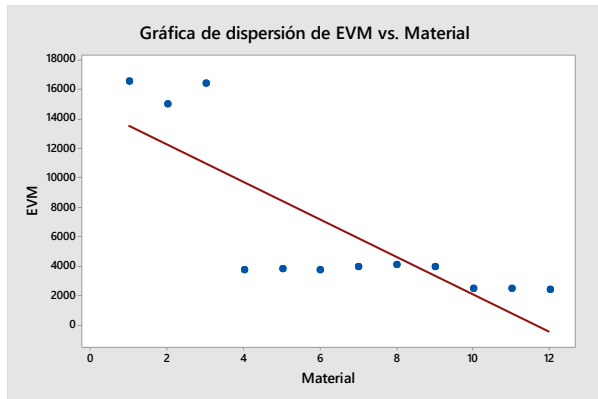
Figure 11

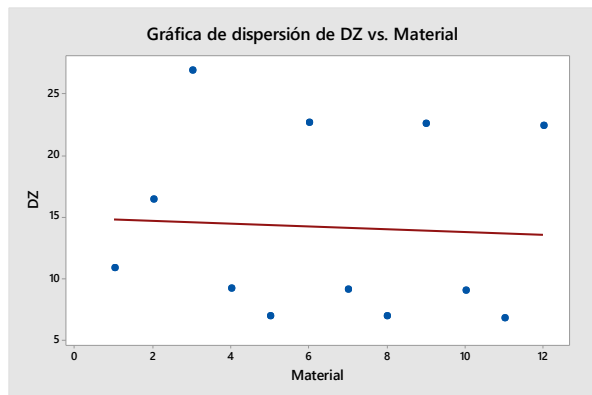Scatter plot for the variable Von Mises Stress (VMS)

Source: Own elaboration

Figure 11
Source: Own elaboration

Figure 10 shows that specimens 8, 9 and 10 received the highest acceptance in the simulation, as indicated by the dispersion fit.
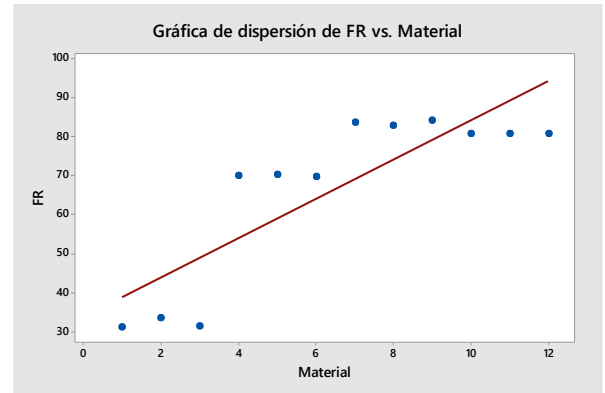
Box 26

Figure 12

Scatter plot for the variable Displacement (DZ)

Source: Own elaboration

In Figure 11, specimen number 2 also shows the best behavior, since it presents the smallest displacement.

Figure 12 shows the behavior of the material in relation to the reaction force at the time of the simulation.

Box 27

Figure 13

Scatter plot for the variable Reaction Effort (RF)

Source: Own elaboration

The specimens showing the best performance in relation to reaction force during the simulation with FEM are numbers 6, 9 and 10, as observed in the scatter in Figure 13.

Finally, the deformation variable experienced by the bolt when applying a torque of 1600 Nmm is considered.

Box 28
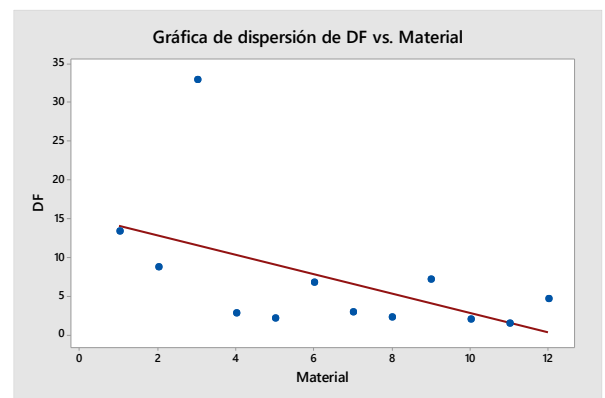
Figure 14

Scatter plot for the variable deformation
Source: Own elaboration

From Figure 14 it can be observed that there is a greater number of specimens that satisfactorily comply with an acceptable percentage in the dispersion for a second evaluation, when related to other variables. In this sense, specimens 1, 6, 10 and 11 meet the objective established for dispersion.

González-Sosa, Jesús Vicente, Avila-Soler, Enrique and Zavala-Osorio, Yadira. [2024]. Optimization of the finite element meshing for the fabrication of a M3x12x0.5 screw, in 3D printing. Journal of Experimental Systems. 11[30]-1-14: e51130114. https://doi.org/10.35429/JOES.2024.11.30.1.14

Journal of Experimental Systems
Article

From a statistical perspective, the specimens that meet the requirements are presented in Table 16. This table also includes the satisfactory results obtained from the simulation with the finite element method (FEM). This information allows us to identify the best option for the evaluation of the screw.

Box 29

Table 16

Optimal simulation and statistical data

		EVM	DZ	FR	DF
1	FEM				
	Estadístico				👍
2	FEM				
	Estadístico		👍		
3	FEM				
	Estadístico				
4	FEM				
	Estadístico				
5	FEM				
	Estadístico				
6	FEM				
	Estadístico			👍	👍
7	FEM			👍	
	Estadístico				
8	FEM			👍	
	Estadístico	👍			
9	FEM			👍	
	Estadístico	👍		👍	
10	FEM	👍	👍		👍
	Estadístico	👍		👍	👍
11	FEM	👍	👍		👍
	Estadístico				👍
12	FEM	👍	👍		👍
	Estadístico				

Source: Own elaboration

According to what is shown in Table 16, the specimens that present the best results in both evaluations, both in the FEM and statistical analysis, are numbers 10 and 11, which correspond to the ABS and Nylon 6/6 material, with a twist angle of 30° and arranged in a linear fashion.

The use of the FEM tool on a screw has the advantage of optimizing and accelerating the evaluation process in order to improve the manufacturing conditions of the screw. In addition, it allows to obtain comparative values in the simulation that are validated, to a certain extent, by statistical tools.

Discussion

In the discussion of recent studies, the growing importance of advanced methodologies in the simulation and fabrication of materials is emphasized. Tian et al. (2024) highlight that generating high-fidelity models is fundamental for achieving precise finite element simulations in composite materials. Their innovative meshing methodology, which utilizes micro-computed tomography (μCT) and neural networks, represents a significant advancement in automation and accuracy in modeling, potentially reducing preparation times and increasing reproducibility of models. This approach not only enhances mesh quality but also expands the possibilities for analyzing complex structures.

On the other hand, Jemal et al. (2024) investigate perforated metals and their optimization in bending processes, addressing the impact of variables such as bend angle and thickness on material behavior. Their findings suggest that perforation geometry has a considerable effect on elastic recovery, highlighting the importance of considering these factors in the design of metal components. This research contributes not only to understanding the behavior of aluminum alloys but also offers a framework for future optimizations in manufacturing processes.

In the healthcare sector, Om et al. (2024) underscore the use of Additive Manufacturing techniques for creating orthopedic braces. Their focus on determining optimal dimensions demonstrates how the integration of simulations and data analysis can enhance the functionality and comfort of medical devices. This study is a clear example of how modern engineering can adapt to the specific needs of patients, paving the way for personalized solutions in medical treatment.

Su et al. (2024) present an innovative approach using the adaptive scaled boundary finite element method (SBFE) to optimize structures that must withstand dynamic loads. The use of advanced adaptive meshing techniques and their ability to handle variable volumes reinforce the need to integrate dynamic simulation in structural design. This approach promises improved efficiency in optimization processes, allowing for more robust and adaptable designs under changing conditions.

Finally, Ho et al. (2024) explore the combination of topology optimization and additive manufacturing in creating continuous carbon fiber composite structures. The significant increases in stiffness achieved with different resins testify to how research in materials and manufacturing techniques can lead to drastic improvements in structural performance. The analysis of microstructures also provides crucial insights into material behavior, which can inform future design iterations.

Collectively, these studies reflect a trend toward the integration of advanced techniques in design and manufacturing, underscoring the importance of innovation in engineering to address contemporary challenges across various industries. The synergy between precise simulations, process optimization, and customization in manufacturing promises to revolutionize how materials and components are designed and produced in the future.

Conclusions

The manufacture of an M3x12x0.3 screw by 3D printing represents an innovative alternative in the design and production of mechanical components. This analysis focuses on the evaluation of bolt performance under specific loads using FEM. Through computer simulations, it is possible to determine how the material and dimensions of the screw affect its mechanical behavior, thus providing a deeper understanding of its functionality and limitations. The integration of scatter plots to visualize Von Mises stress, displacement, strain and reaction stress allows discerning relevant patterns and trends in the structural analysis of the bolt.

In the Von Mises stress evaluation, the results obtained illustrate how the bolt behaves under applied loading conditions. The scatter plots show that, even if the bolt is designed to withstand certain applied loads, there is a critical threshold beyond which the material begins to yield. This type of analysis is crucial as it allows to accurately identify the safe operating range of the screw, avoiding potential failures that could compromise the integrity of the systems in which it is integrated. Interpretation of these graphs helps to understand the importance of careful design with respect to the direction the head should take for screw production.

Displacement and deformation are other key parameters analyzed in this research. By examining the results obtained, it is evident that the screw presents an elastic behavior within a specific range of loads, which suggests that 3D printing of the screw allows a structure with certain recovery capabilities under transient loads. However, it was observed that the displacement increases significantly with increases in load, indicating a possible limitation in applications where extreme stiffness is required. Scatter plots clearly reflect this relationship, facilitating design adjustments to improve performance.

On the other hand, the reaction stress is a fundamental aspect in the evaluation of the load capacity of the bolt. Through simulation, it was possible to identify the critical areas where the greatest stresses are concentrated, which points to potential points of failure. This phenomenon not only highlights the importance of structural analysis in screws manufactured by 3D printing, but also suggests the possibility of optimizing the design by modifying the geometry or choosing more appropriate materials. The visualization of this information becomes a valuable tool for engineers seeking to innovate in the use of bolts in various applications.

Finally, the analysis and evaluation of the M3x12x0.3 screw manufactured with 3D printing highlights the relevance of employing tools such as FEM and scatter plots to make informed mechanical design decisions. This study not only provides an in-depth understanding of the mechanical behavior of the screw, but also highlights the potential of 3D printing in the manufacture of high-precision components. As we continue to advance 3D printing technology, new opportunities will open up to optimize designs, improve materials and, consequently, raise engineering quality and performance standards. The conclusion of this analysis serves as a starting point for future studies that delve deeper into the interplay between materials, design and 3D printing in the creation of advanced mechanical components.

Annexes

Tables and adequate sources.

González-Sosa, Jesús Vicente, Avila-Soler, Enrique and Zavala-Osorio, Yadira. [2024]. Optimization of the finite element meshing for the fabrication of a M3x12x0.5 screw, in 3D printing. Journal of Experimental Systems. 11[30]-1-14: e51130114.
https://doi.org/10.35429/JOES.2024.11.30.1.14

Declarations

Conflict of interest

The authors declare no interest conflict. They have no known competing financial interests or personal relationships that could have appeared to influence the article reported in this article.

Author contribution

González-Sosa, Jesús Vicente: Contributed to the project idea, research method and technique.

Avila-Soler, Enrique: Contributed to the project idea, research method and technique.

Zavala-Osorio, Yadira: Contributed to the project idea, research method and technique.

Availability of data and materials

The data obtained was derived from modeling and measurement data with metrological instruments.

Funding

Acknowledgements

Abbreviations

FEM	Finite Element Method
MAI3D	manufacturing with 3D printing
I3D	3D printing
ABS	Butadiene Styrene
PLA	Polylactic Acid
MF	Flexural Modulus
DF	Deformation
EF	Stress

References

Antecedents

Çetin, A., & Bircan, D. A. [2021]. 3D pull-out finite element simulation of the pedicle screw-trabecular bone interface at strain rates. Proceedings of the Institution of Mechanical Engineers, Part H: Journal of Engineering in Medicine, 236(1), 134–144.

Chandra, G., & Pandey, A. [2021]. Design and analysis of biodegradable buttress threaded screws for fracture fixation in orthopedics: a finite element analysis. Biomedical Physics & Engineering Express, 7(4), 045010.

Hsia, S.-Y., Chou, Y.-T., & Lu, G.-F. [2016]. Analysis of Sheet Metal Tapping Screw Fabrication Using a Finite Element Method. Applied Sciences, 6(10), 300.

Figueroa Díaz, R. A., Balvantín García, A. de J., Diosdado de la Peña, J. Á., Cruz Alcantar, P., Murillo Verduzco, I., & Pérez Olivas, P. A. [2019]. Stress analysis in a screw conveyor axis under a specific fault condition. Ingeniería Investigación y Tecnología, 20(3), 1–11.

Lee, S. H., Hong, M. H., & Lee, K. B. [2017]. Finite Element Analysis of Screw-Tightening Torque Applied to Custom and Conventional Abutment. Global Journal of Health Science, 9(9), 165.

Sheng, W., Ji, A., Fang, R., He, G., & Chen, C. [2019]. Finite Element- and Design of Experiment-Derived Optimization of Screw Configurations and a Locking Plate for Internal Fixation System. Computational and Mathematical Methods in Medicine, 2019, 1–15.

Xue, H., Zhang, Z., Liu, M., Lin, Z., Endo, Y., Liu, G., Mi, B., Zhou, W., & Liu, G. [2022]. Finite element analysis of different fixation methods of screws on absorbable plate for rib fractures. Frontiers in Bioengineering and Biotechnology, 10.

Zhu, Y., Babazadeh-Naseri, A., Dunbar, N. J., Brake, M. R. W., Zandiyeh, P., Li, G., Leardini, A., Spazzoli, B., & Fregly, B. J. [2023]. Finite element analysis of screw fixation durability under multiple boundary and loading conditions for a custom pelvic implant. Medical Engineering & Physics, 111, 103930.

Discussions

Ho, T. N. T., Nguyen, S. H., Le, V. T., & Hoang, T. D. [2024]. Coupling design and fabrication of continuous carbon fiber-reinforced composite structures using two-material topology optimization and additive manufacturing. The International Journal of Advanced Manufacturing Technology, 130(9), 4277-4293.

Jemal, A., Salau, A. O., & Wondimu, A. [2024]. Finite element method–based multi-objective optimization of press-brake bending of sheet metal. The International Journal of Advanced Manufacturing Technology, 130(9), 4263-4275.

Om, M. S., Yang, W. C., Choe, C. M., Kim, U. H., Ri, W. S., & Sok, S. H. [2024]. A reasonable approach to determine structural dimension of FDM fabricated orthopedic orthosis using finite element simulation and simple additive weighting method. Proceedings of the Institution of Mechanical Engineers, Part C: Journal of Mechanical Engineering Science, 09544062241282496

Su, R., Zhang, X., Tangaramvong, S., & Song, C. [2024]. Adaptive scaled boundary finite element method for two/three-dimensional structural topology optimization based on dynamic responses. Computer Methods in Applied Mechanics and Engineering, 425, 116966.

Tian, X., Zhang, H., Qu, Z., & Ai, S. [2024]. An efficient finite element mesh generation methodology based on μCT images of multi layer woven composites. Composites Part A: Applied Science and Manufacturing, 184, 108255.

Article

SiO₂/PDMS modified porous systems for oil removal: reuse cycles studied

Modificación de sistemas porosos con SiO₂/PDMS como removedores de aceite: estudio de ciclos de reúso

Salazar-Hernández, Carmen*[a], Salazar-Hernández, Mercedes[b], Mendoza-Miranda, Juan Manuel[c] and León-Reyes, María del Rosario[d]

[a] ROR Instituto Politécnico Nacional-UPIIG • D-4418-2019 • 0000-0002-6901-2937 • 105461
[b] ROR Universidad de Guanajuato • LTF-1226-2024 • 0000-0001-8039-8124 • 446271
[c] ROR Instituto Politécnico Nacional-UPIIG • LTF-7054-2024 • 0000-0003-4777-767X • 295057
[d] ROR Instituto Politécnico Nacional-UPIIG • 0000-0002-9848-1070 • 210207

Abstract

Currently, water pollution is a global problem that must be addressed; since, added to the aridity cycles, they have caused a shortage of natural water resources. Therefore, improving wastewater treatment methods is a global research topic that needs to be developed. Among the contaminants present in wastewater (industry and domestic) are "oily substances" which are dispersed in the water, making their removal difficult. Therefore, this project seeks to determine the reuse capacity for an oily substance removal system designed from the modification of a porous medium with a hydrophobic ceramic (SiO₂/PDMS) that contains in the structure of the siloxane chain the methyl functional group (-CH₃). To do this, the liquid-liquid extraction of the oil removed from the sponge/ceramic was carried out using solvents such as: hexane and THF; determining the numbers of use cycles, identifying by infrared spectroscopy the modifications in the modified sponge after each use cycle.

Resumen

En la actualidad, la contaminación del agua es un problema mundial que debe ser atendido; ya que sumado a los ciclos aridez han provocado una escases del recurso hídrico natural. Por lo que mejorar los métodos de tratamiento de aguas residuales es un tema de investigación mundial necesario por desarrollar. Entre los contaminantes presentes en las aguas residuales (industria y doméstica) se encuentra las "sustancias oleosas" las cuales se dispersan en el agua dificultando su remoción. Por lo que, en este proyecto se busca determinar la capacidad de re-uso para un sistema de remoción de sustancia oleosas diseñado a partir de la modificación de un medio poroso con un cerámico hidrofóbico (SiO₂/PDMS) que contiene en la estructura de la cadena siloxana el grupo funcional metilo (-CH₃). Para ello, se realizó la extracción líquido-líquido del aceite removido en la esponja/cerámico empleando disolventes tales como: hexano y THF; determinando los números de ciclos de uso identificando por espectroscopia de infrarrojo las modificaciones en la esponja modificada después de cada ciclo de uso.
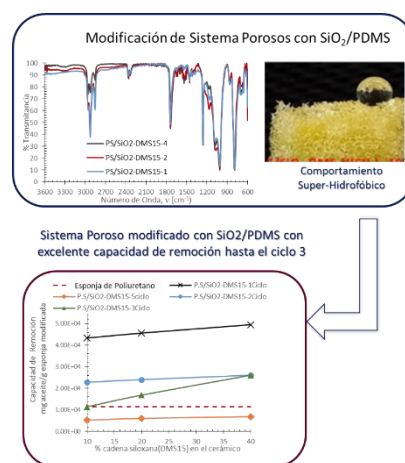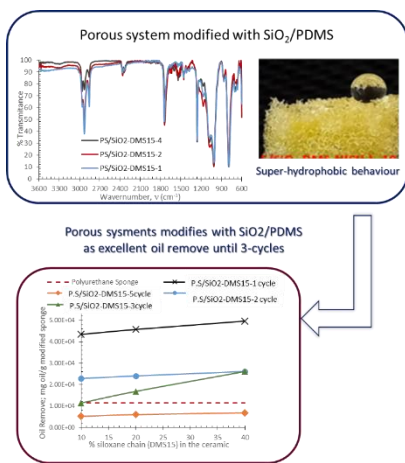
SiO2/PDMS, Oil remotion, Reuse-cycles

SiO2/PDMS, Remoción de aceite, Ciclos de reúso

RENIECYT
Registro Nacional de Instituciones y Empresas Científicas y Tecnológicas
1702902 CONAHCYT

Introduction

The use of adsorbent systems as a means for the removal of contaminants represents a highly efficient alternative, allowing for the elimination of various types of contaminants through the control of the interactions between the sorbate and the adsorbent. In this regard, mesoporous silica is an inorganic solid with a structured pore network and high adsorption capacity (Technologies, 2024; Seisenbaeya G.A; et.al 2021; Ulfa M, et.al 2022; Flores D, et.al, 2022). It has been demonstrated that a range of contaminants, including heavy metals (Grozdov D, et.al 2023; Zhu W, et.al 2017; Nicola R, et. al 2020), dyes chlorinated compounds (Quin Q, et.al, 2012),, and pesticides (Kong X.P, et.al 2021), can be efficiently adsorbed on these materials, with removal efficiencies ranging from good to excellent (Palomino J.M, 2014, Wu Z, et.al, 2011).

On the other hand, silica offers the advantage of straightforward functionalization of the surface. Figure 1 demonstrates that, through reactions with the silanol groups present on the surface, condensation reactions can be conducted with alkylalkoxysilanes, enable the addition of diverse molecular types (Ghosh S, et. al, 2013; Tian J, et. al. 2015). These groups include amino, thiol, and alkyl groups, as well as proteins, sugars, enzymes, and molecular recognizers (Kucinski K, et. al 2018). As a result, they can be used as selective adsorbents in a variety of fields, including metallurgy (Salazar-Hernández M, 2024), pharmaceuticals (jaafar J.A, et. al, 2019; Kirla H, et. al, 2023), and the environment (Xu P, et.al, 2018; Song Y, et.al, 2019; Abdulazeez I, et. al, 2023).

Box 1
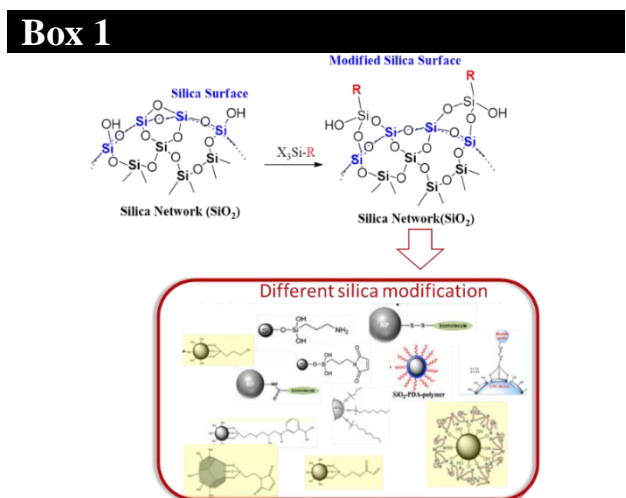
Figure 1

Modification of the silica surface with different functional groups

Table 1 provides an overview of the environmental applications of silica modified with alkyl (–R) groups, which impart hydrophobic characteristics. These materials have been employed for the removal of a range of pollutants, including Cu(I), Cd (II), Pb(II), Active Red X-3B, and rhodamine B, as well as organic solvents such as phenol, toluene, trichloroethylene, and chlorobenzene, as well as oil and fatty substances. To achieve the removal of contaminants, hydrophobic silica is deposited on matrices such as cellulose, chitosan, carbon nanotubes, graphene oxide, and others (Salazar-Hernández C, et.al, 2021; Gómez-López R.V, et.al 2022).

Box 2

Table 1

Environmental applications of hydrophobic silica (Gómez-López R.V, 2022)

| Applications	Silica deposition matrix	Adsorbate	Removal
Removal of metal and organic contaminants	Cellulose-silica aerogel	Cu (I)	801 mg/g
	RC-base aerogel	Cd(II)	100.16 mg/g
		Pb(II)	152.23 mg/g
	Chitosan	Pb(II)	102.03 mg/g
	Cellulose-chitosan	Active red X-3B	100%
	CNT and chitosan	Chipton	227.3 mg/g
	Graphene Oxide	Fenol	99%
	cellulose	Rhodamine B	97%
Organic Solvents and oil removal	CF$_3$ Functionalized	oil	Absorbs 14 times more oil than Aerogel weighs
	Reduced Graphene Oxide	Fatty substance	4517-14728%w
	Cellulose-silica hybrid	Fatty substance	24.8 g/g
	TFPTMOS y TMOS	Toluene	833 mg/g
		Ethanol	458 mg/g
		Chlorobenzene	11890 mg/g
		Trichloroethylene	1935 mg/g

Source: Own elaboration

In this context, Salazar-Hernandez et al. have developed a modification of the silica surface with different organic functional groups, including methyl, octyl, and polysiloxane (PDMS), which has been observed to increase the hydrophobic character as follows: SiO$_2$ < SiO$_2$–CH$_3$ < SiO$_2$–octyl < SiO$_2$–PDMS.

The results showed that the hydrophobic character of the modified silica serves to control the oil removal capacity through flocculation, resulting in a maximum for the SiO$_2$/PDMS system of 4 g oil/g SiO$_2$–PDMS (Gómez-López R.V, et. al, 2022). The feasibility of using a porous system (polyurethane sponge) as a removal system for oily substances was determined by modifying it with the SiO$_2$/PDMS ceramic. Figure 2 illustrates the contaminant removal capacity, demonstrating a removal capacity of 10 g of oil per m² of treated sponge, which is equivalent to 12.25 g oil/g of modified sponge (Gómez-López, R.V, et. al, 2022; Feng X, et. al 2024).

Box 3
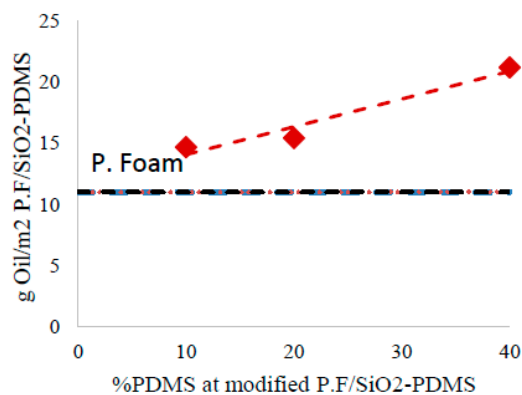
Figure 2

Oil removal capacity for P.F/SiO$_2$-PDMS
Source: Take from Gómez-López R.V, et.al 2022

Thus, this study aims to present the removal capacity of foam modified with ceramic in different contaminant removal-extraction cycles.

Experimental procedure

Synthesis of SiO$_2$/PDMS and the modification of polyurethane

The silica modification was conducted via co-condensation, as previously reported by Salazar–Hernandez et al 2021. The polymerization of TEOS (Aldrich; 99%) is conducted by magnetic stirring for 30 minutes at 50 °C, with the addition of PDMS (Gelest) and DBTL as a polycondensation catalyst. Table 2 provides a detailed account of the concentrations of PDMS used in the silica modification process. The polyurethane sponge (5 mm x 3 mm x 2 mm) was subjected to impregnation, after which it was dried at 50°C for 24 hours.

Box 4

Table 2

Amounts of TEOS/PDMS used for silica modification.

	TEOS (g)	PDMS (g)
SiO$_2$/DMS15-1	10	1
SiO$_2$/DMS15-2	10	2
SiO$_2$/DMS15-4	10	4

Characterization of the ceramic-modified sponge

ATR-FT. Attenuated total reflection Fourier transform spectroscopy (ATR-FT) was employed to obtain the infrared spectra. This was conducted using a Nicolet iS10 spectrometer from Thermo Scientific, with an average of 16 scans acquired across a spectral window of 4000–600 cm^{-1} and a resolution of 4 cm^{-1}.

Hidrophobicity-Contact Angle. The contact angle for the sponge and sponge-modified was determined using a drop of distilled water from L. The image was captured with a conventional cell camera and the contact angle was measured with the free software IC-Measure, with the horizontal base serving as the reference point.

Oil removal test. The oil absorption process was initiated by adding 20 mL of water with red vegetable dye at a concentration of 0.001% (vol./vol.) to a beaker containing 2 mL of vegetable oil (commercial vegetable oil). This mixture was prepared as an emulsion in synthetic water to facilitate experimentation. The modified sponge was then introduced into the emulsion to determine the quantity of oil removed, with measurements taken with a test tube.

Oil extraction procedure. The organic solvent was added for oil extraction, with the extraction cycles conducted with constant agitation for five minutes in an orbital shaker. Thereafter, the solution was allowed to drain, and it was subsequently dried in an oven at 80°C for 24 hours to eliminate the impregnated solvent. Subsequently, the structural modification of the material was assessed through the evidence of its infrared spectra.

Salazar-Hernández, Carmen, Salazar-Hernández, Mercedes, Mendoza-Miranda, Juan Manuel and León-Reyes, María del Rosario. [2024]. SiO2/PDMS modified porous systems for oil removal: reuse cycles studied. Journal of Experimental Systems. 11[30]-1-9: e61130109.
DOI: https://doi.org/10.35429/JOES.2024.11.30.6.9

Results and discussions

*Sponge modified with SiO₂/PDMS ceramics*

Figure 3a shows the infrared spectrum for the unmodified sponge. It shows the characteristic functional groups for polyurethane at 1650 cm^{-1} and 1708 cm^{-1}. It also shows the N–H at 3294 cm^{-1} and the C–O–C at 1094 cm^{-1}. C at 1094 cm^{-1}, C–H at 2966–2867 and 1440 cm^{-1}, C–N at 1020–1220 cm^{-1}, C=C at 1603, 1580 cm^{-1}. Figure 3b shows that this material is hydrophilic, meaning it wets out easily.

Upon modification with the ceramic (Figure 3c), the signals of the impregnated foam are identified. At 1100 and 790 cm^{-1}, the Si–O–Si network is observed, while at 1200 cm^{-1}, the Si–C group of the siloxane chain is observed at 900 cm^{-1}, showing as an intense and sharp band. Additionally, the Si-O-Si group of the siloxane chain is discernible at this same wavelength, revealing a distinct and prominent peak. Finally, the C–H of the –CH₃ is evident at 2900 cm^{-1}. On the other hand, it was observed that the sponge underwent further modification as the DMS15 content in the ceramic increased. Furthermore, the ceramic induces a transition from hydrophilic to hydrophobic behavior in the sponge (Figure 3d), as evidenced by a modification of the contact angle to a value of 136–140° in accordance with the increase in the siloxane chain length within the silica network. The results suggest an excellent modification of polyurethane sponge with ceramic SiO2/PDMS according to previous reports of this hybrid ceramic (Feng X, et. al, 2024; Chen K, et. al, 2024; Xu S, et. al 2024)

Box 5

a)
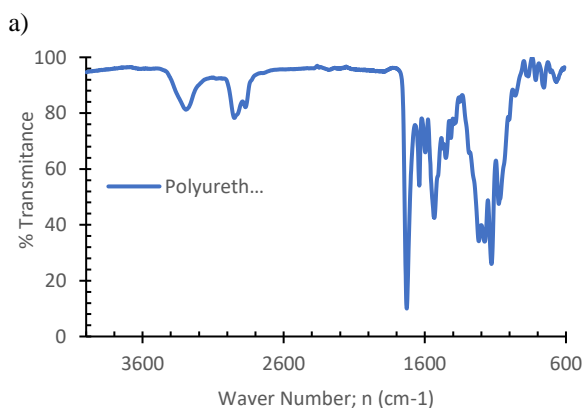
b)
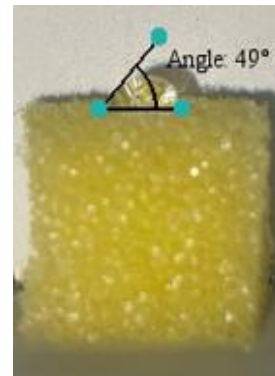
c)
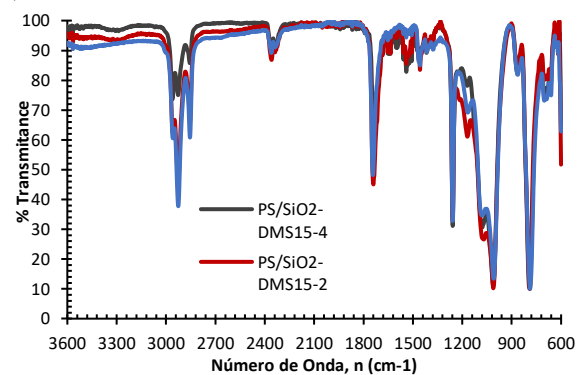
d)

Figure 3

Characterization of the polyurethane sponge (a) infrared spectrum before modification (b) contact angle before modification (d) infrared spectrum modified with the ceramic (e) contact angle after modification with ceramic

Figure 4 shows the effect of siloxane chain content on the hydrophobicity of the material, as indicated by the contact angle (θ). The data demonstrate that an increase in the DMS15 content in the ceramic resulted in a corresponding increase in the contact angle. Specifically, the ceramic with 40% DMS15 exhibited a contact angle of 141°, while the ceramic with 10% DMS15 displayed a contact angle of 136.75°. Conversely, the data indicates that the ceramics exhibit superhydrophobic characteristics (Zhou E, et. al, 2024), as evidenced by a contact angle exceeding 120° (Danish M, 2022).

Journal of Experimental Systems

Article

Box 6
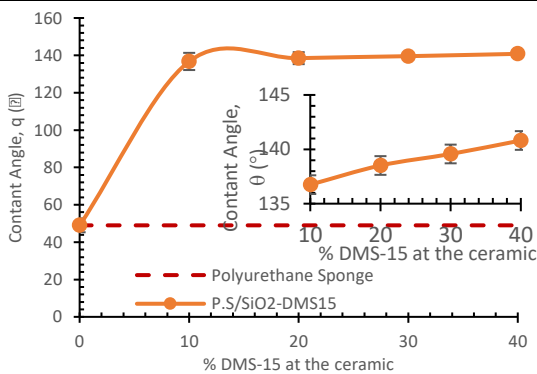
Figure 4

Effect of siloxane chain content (DMS15) in the silica network on hydrophobic behavior

Oil Removal Tests

Reuse Cycles

Figure 5 shows how well the unmodified sponge, and the sponge modified with different siloxane chain contents (DMS15) remove oil. The unmodified sponge can only be used once because the oil gets in between its pores. To choose the best solvent for extraction, we tested three common solvents: kerosene, THF, and hexane. We found that hexane was the most effective at removing the oil, with a recovery percentage of 45-50%. Hermogenes et al. 2010 have found this organic solvent works well for extraction, even though it has a moderate recovery percentage.

Box 7

Table 3

Oil extraction capacity in water with organic solvents

	% Oil recovery
Kerosene	20
THF	40
Hexane	45–50

The results demonstrated that the higher the DMS15 content in the ceramic, the greater the removal capacity. Table 4 shows the increase in the removal of the modified sponges in each cycle. In the first cycle, for example, the removal capacity was 1.7 times greater for the sponge modified with the ceramic containing 10% of the siloxane chain (DMS15) than for the control sponge.

In the initial cycle, the sponge modified with the ceramic containing 10% of the siloxane chain (DMS15) exhibited an increase of 3.8 times, while the DMS15 content was increased to 40% in the subsequent cycle, resulting in a 4.5 increase.

Box 8

Table 4

Oil removal capacity of the modified sponge

	Removal Cycle			
	1	2	3	5
Polyurethane Sponge	1	---	---	---
SP/SiO2-DMS15-1	3.8	2	1	0.46
SP/SiO2-DMS15-2	4	2.10	1.52	0.52
SP/SiO2-DMS15-4	4.5	2.3	2.28	0.62

Box 9
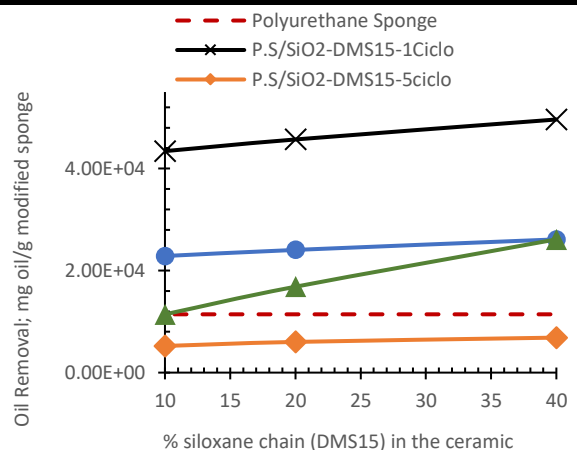
Figure 5

Oil removal capacity of the SiO2/DMS15 modified sponge with varying siloxane chain content.

Figure 6 shows the corresponding spectra for the modified sponge following the initial and second removal cycles. In the second removal cycle, the sponge exhibited a notable loss in its adsorption capacity, reaching approximately 50% as observed in Figure 6b. Following the initial removal cycle, the ceramic remained unaltered in its structural composition, with the exception of a reduction in the intensity of the bands at 1200 cm^{-1} (Si–C). The spectra also show a decrease in the intensity of the Si–C band at 1200 cm^{-1}, which is attributed to the removal of the siloxane chain, and an increase in the intensity of the Si-O-Si band at 1100 cm^{-1}, which is associated with the formation of a silica network. Additionally, there is an observed increase in the intensity of the C–H band between 2800 and 2900 cm^{-1}, which may suggest the presence of a thin layer of oil that is not fully extracted from the system. This could explain the observed decrease in the observed removal capacity.

Salazar-Hernández, Carmen, Salazar-Hernández, Mercedes, Mendoza-Miranda, Juan Manuel and León-Reyes, María del Rosario. [2024]. SiO2/PDMS modified porous systems for oil removal: reuse cycles studied. Journal of Experimental Systems. 11[30]-1-9: e61130109.
DOI: https://doi.org/10.35429/JOES.2024.11.30.6.9

In the third cycle, the removal capacity decreases by approximately 70%. According to the infrared spectrum after the second cycle (Figure 6c), the oil layer retained in the ceramic sponge is predominant, with the signals corresponding to the ceramic (1200 cm^{-1} and 1100 cm^{-1}) observed with very low intensity. In subsequent cycles, the quantity of oil is markedly elevated, and the presence of ceramic is no longer evident.

Hexane is inadequate for the complete extraction of the oily substance. Consequently, a residual layer is retained from the initial cycle, which increases with each subsequent cycle, thereby reducing the removal capacity. The functional use of the removal system is limited to up to five cycles.

Box 10

a)

b)

c)

d)
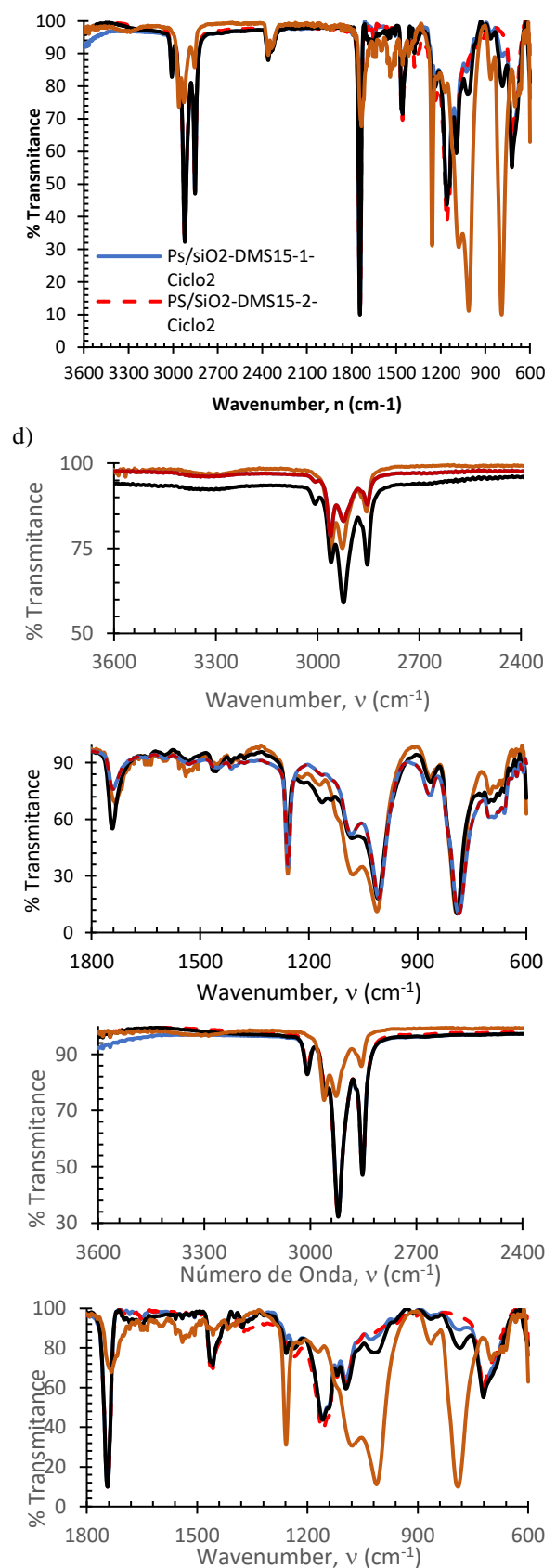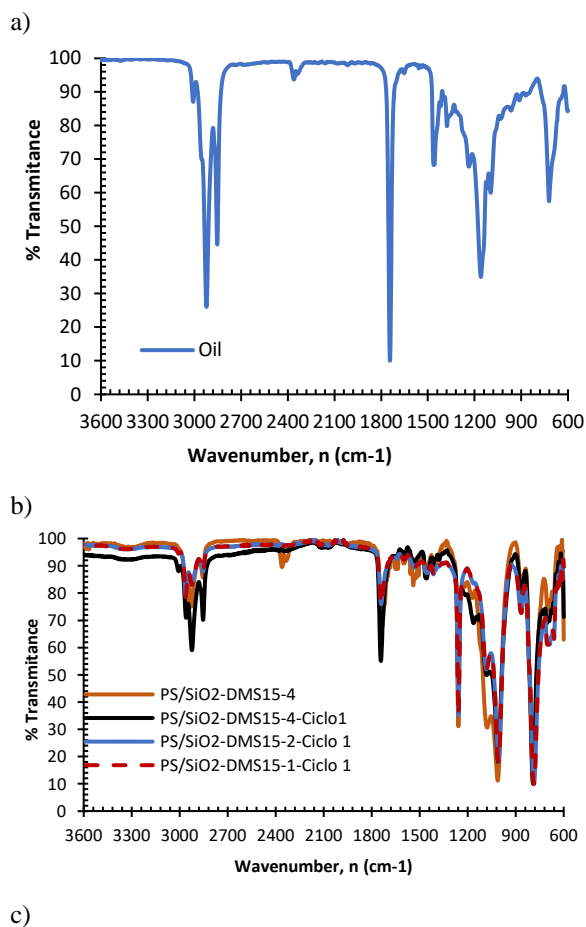
Figure 8

Modification of PS/SiO₂–DMS15 after each removal cycle (a) vegetable oil (b) first cycle (b) second cycle

Salazar-Hernández, Carmen, Salazar-Hernández, Mercedes, Mendoza-Miranda, Juan Manuel and León-Reyes, María del Rosario. [2024]. SiO2/PDMS modified porous systems for oil removal: reuse cycles studied. Journal of Experimental Systems. 11[30]-1-9: e61130109.
DOI: https://doi.org/10.35429/JOES.2024.11.30.6.9

Conclusions

The modification of adsorption systems, such as the polyurethane sponge, with hydrophobic ceramics (SiO₂/PDMS-CH₃), has been demonstrated to enhance the retention capacity of oily agents, including oil. Nevertheless, a significant challenge inherent to any method of contaminant removal is the effective extraction and recovery of the contaminant from the extractant medium.

Despite the use of an organic solvent related to oil (hexane), the recovery of the dispersed oil in water was found to be only 45–50%. Consequently, based on the infrared spectra obtained for the PS/SiO₂–DMS15–CH₃ from the initial cycle, a minimum layer of oil is retained, and its concentration increases with each subsequent cycle. This results in a gradual decrease in the contaminant removal capacity.

The optimal number of cycles for use-reuse of the PS/SiO₂–DMS15–CH₃ system is five. This is based on the observation that under the extraction conditions used, the concentration of oil in water is significantly higher than that found in wastewater. Consequently, the time of use and application of these systems can be highly effective and low cost.

Acknowledgements

Statements & declarations

Consent to participate and Consent for publication

The authors express their approval to participate and publish this work in ECORFAN Journal

Conflict of interest

The authors declare no interest conflict. They have no known competing financial interests or personal relationships that could have appeared to influence the article reported in this article.

Author contribution

All authors contributed to the development and revision of the manuscript; CSH and MSH (conceptualization, interpretation and analysis date; writing and financial support); JMMM (interpretation and analysis date and methodology), MRLR (interpretation and acquisitions date). All authors read and approved the final manuscript.

Availability of data and materials

Indicate the availability of the data obtained in this research.

Funding

Abbreviations

SiO₂	Silica ceramic
PDMS	Polydimethylsiloxane
SiO₂/PDMS	Silica ceramic modified with polydimethylsiloxane
SiO₂/DMS15-1	Silica ceramic modified with 10 % weight polydimethylsiloxane
SiO₂/DMS15-2	Silica ceramic modified with 20 % weight polydimethylsiloxane
SiO₂/DMS15-4	Silica ceramic modified with 40 % weight polydimethylsiloxane
P.S	Polyurethane sponge
	Contact angle

References

Antecedents

Flores D, Almeida C.M.R, Gomes C.R, Balula S.S, Granadeiro C.M, Tailoring of mesoporous silica base materials for enhanced water pollutants removal, Molecules (2023) 28(10) 4038.
https://doi.org/10.3390/molecules28104038

Grozdov D, Zincovscaia I, Mesoporous materials for metal-laden wastewater treatment, Materials (Basel) (2023) 16(17) 5864. doi: 10.3390/ma16175864

Kong X.P, Zhang B.H, Wang J, Multiple roles of mesoporous silica in safe pesticide application by nanotechnology: A review, Journal of Agricultural and Food Chemistry (2021) 69 (24) 6735-6754. https://doi.org/10.1021/acs.jafc.1c01091

Nicola R, Muntean S.G, Nistor M.A, Putz A.M, Almásy L, Sacarescu L, Highly efficient and fast removal of colored pollutants from single and binary systems, using magnetic mesoporous silica, Chemosphere (2020) 261, 127737. https://doi.org/10.1016/j.chemosphere.2020.127737

Optimización del tratamiento de aguas residuales industriales en México: regulación más estricta y escases de agua. Recuperado 20/02/2024. https://es.genesiswatertech.com/blog-post/optimizing-industrial-wastewater-treatment-in-mexico/

Palomino J.M, Tran D.T, Hauser J.L, Dong H, Oliver S.R:J, Mesoporous silica nanoparticles for high capacity adsorptive desulfurization, Journal of Materials Chemistry A (2014) 2, 14890-14895. https://doi.org/10.1039/C4TA02570A

Qin Q, Liu K, Fu D, Gao H, Effect of chlorine content of chlorophenols on their adsorption by mesoporous SBA-15, Journal of Environmental Sciences (2012) 24(8) 1411-1417. https://doi.org/10.1016/S1001-0742(11)60924-8

Seisenbaeva G.A, Ali L.M.A, Vardanyan A, Gary-Bobo M, Budnyak T, Kessler V.G, Durand J.O, Mesoporous silica adsorbents modified with aminopolycarboxylate ligands functional characteristics, health and environmental effects (2021) Journal of Hazardous Materials, 406, 124698. Doi.org/10.1016/j.jhazmat.2020.124698

Ulfa M, Prasetyoko D, Trisunaryanti W, Bahruji H, Fadila Z.A, Sholeha N.A, The effect of gelatin as pore expander in green synthesis mesoporous silica for methylene blue adsorption, Scientific Reports (2022) 12, 15271. https://doi.org/10.1038/s41598-022-19615-5

Wu Z, Zhao D, Ordered mesoporous materials as adsorbents, Chemical Communications (2011) 47, 3332-3338. https://doi.org/10.1039/C0CC04909C

Zhu W, Wang J, Wu D, Li X, Luo Y, Han C, Ma W, He S, Investigating the heavy metal adsorption of mesoporous silica materials prepared by microwave synthesis, Nano Research Letter (2017) 12; 323. https://doi.org/10.1186/s11671-017-2070-4

Basics

Ghosh S, Goswami S.S, Mathias L.J, Surface modification of nano-silica with amides and imides for use in polyester nanocompositest, Journal of Chemestry A (2013) 1, 6073-6080. DOI: 10.1039/c3ta10381a.

Jaafar J.A, Kamarudin N.H.N, Setiabudi H.D, Timmiati S.N, Peng T.L, Mesoporous silica nanoparticles and wast derived-siliceous materials for doxorubicin adsorption and release, MaterialsToday Proceedings (2019) 19(4) 1420-1425. https://doi.org/10.1016/j.matpr.2019.11.163

Kirla H, Henry D.J, Jansen S, Thompson P.L, Hamzah J, Use of silica nanoparticle for drug delivery in cardiovascular disease, Clinical Therapeutics (2023) 45(11) 1060-1068. https://doi.org/10.1016/j.clinthera.2023.08.017

Kucinski K, Jankowska-Wajda M, Ratajczak T, Balabanska-Trybus S, Schulmann A, Maciejewski H, Chmielewski M, Hreczycho G, Silica surface modification and its application in permanent link with nucleic acids, ACS-Omega (2018) 6, 5931-5937. https://doi.org/10.1021/acsomega.8b00547

Salazar-Hernández M, Salazar-Hernández C, Elorza-Rodrìguez E, Mendoza-Miranda J.M, Puy-Alquiza M.J, Miranda-Aviles R, Rodríguez-Rodríguez C, Using of green silica amine-Fe3O4 modified from recovery Ag(I) on aqueous system, Silicon (2024) 16, 1509-1524 https://doi.org/10.1007/s12633-023-02779-8.

Journal of Experimental Systems

Article

Song Y, Ding Y, Wang F, Chen Y, Jiang Y, Construction of nano-composites by enzyme entrapped in mesoporous dendritic silica particles for efficient biocatalytic degradation of antibiotics in wastewater, Chemical Engineering Journal (2019) 375, 121968. https://doi.org/10.1016/j.cej.2019.121968

Tian J, Zhang H, Liu M, Deng F, Huang H, Wan Q, Li Z, Wang K, He X, Zhang X, Wei Y, A bioinspired strategy for surface modification of silica nanoparticles, Applied Surface Science (2015) 357 Part B, 1996-2003. https://doi.org/10.1016/j.apsusc.2015.09.171

Xu P, Nan Z, Facile synthesis of magnetic hollow mesoporous silica spheres with assembled shell by nanosheets as an excellent adsorbent, Materials Letters (2018) 218, 209-212.
https://doi.org/10.1016/j.matlet.2018.02.022

Suport

Abdulazeez I, Alrajjal A.S, Ganiyu S, Baing N, Salhi B, AbdElazem S, Facile engineering of mesoporous silica for the effective removal of anionic dyes from wastewater: Insights from DFT and experimental studies, Heliyon (2023) 9(11) e21356. https://doi.org/10.1016/j.heliyon.2023.e21356

Gómez-López R.V, Salazar-Hernánez M, Moreno-Palemrín J, Salazar-Hernández C, SiO2-PDMS as oil removal system, Journal of technology and Innovation (2022) 9 (24) p.p. 29-35. DOI: 10.35429/JIT.2022.24.9.29.5

Humbert L, Solid phase extraction (SPE): theory and applications, Annales de Toxicologie Analytique, (2010) 22 (2) 61-68.
Salazar-Hernández C, Salazar-Hernández M, Hernández-Arias LJ, Mendoza-Miranda J.M, Removal of Oil Pollution in water using hydrophobic silica, Journal of Systematic Innovation (2021) 5(16) 2021, 1-5. DOI: 10.35429/JSI.2021.16.5.1.5

Difference

Chen K, Feng X, Guo X, Zhang J, Huang Y, Zhang X, Shang B, Chen D (2024) Water-Soluble, Self-Healing, and Debonding Primer for the Interface between Silicone Leather and Polydimethylsiloxane Composites, Langmuir,

40(22) 11684-11694. https://doi.org/10.1021/acs.langmuir.4c01059

Feng X, Chen K, Guo X, Sun J, Jian Y, Yan W, Qian S, Xu W, Chen D (2024) Structure-property relationship of polyhedral oligomeric silsesquioxanes/polydimethylsiloxane superhydrophobic coatings for cotton fabrics, Progress in Organic Coatings, 192: 108476. DOI: 10.1016/j.porgcoat.2024.108476

Discussion

Danish, M. (2022). Contact Angle Studies of Hydrophobic and Hydrophilic Surfaces. In: Handbook of Magnetic Hybrid Nanoalloys and their Nanocomposites. Springer, Cham. https://doi.org/10.1007/978-3-030-34007-0_24-1

Hermógenes Giraldo Y, Jorge Velásquez J., Paola Cuartas A. Extracción con solventes y purificación de aceite a partir de semillas de jatropha curcas. Revista Investigaciones Aplicadas, (2010) 4(2), 77–86. http://revistas.upb.edu.co/index.php/investigacionesaplicadas/article/view/719

Xu S, Yu Z, Pang Y, Chen Z, Chen Y, Zhang X, Guo S (2024) Advances in the application of superhydrophobic fabric surfaces for oil-water separation and extension of functionalization, Journal of Environmental Chemical Engineering, 12(6) 114156. https://doi.org/10.1016/j.jece.2024.114156

Zhou, E., Shen, Y., Yeerken, A., Jiang, J., Nong, X. (2024). Ice Adhesion on Superhydrophobic Micro-Nanostructure Surfaces. In: Shen, Y. (eds) Icephobic Materials for Anti/De-icing Technologies. Springer, Singapore. https://doi.org/10.1007/978-981-97-6293-4_9

[Title in TNRoman and Bold No. 14 in English and Spanish]

Surname, Name 1st Author*[a], Surname, Name 1st Co-author[b], Surname, Name 2nd Co-author[c] and Surname, Name 3rd Co-author[d] [No.12 TNRoman]

[a] ROR [Affiliation institution](#), ◖ [Researcher ID](#), ⓘ [ORC ID](#), [SNI-CONAHCYT ID](#) or CVU PNPC [No.10 TNRoman]
[b] ROR Affiliation institution, ◖ Researcher ID, ⓘ ORC ID, SNI-CONAHCYT ID or CVU PNPC [No.10 TNRoman]
[c] ROR Affiliation institution, ◖ Researcher ID, ⓘ ORC ID, SNI-CONAHCYT ID or CVU PNPC [No.10 TNRoman]
[d] ROR Affiliation institution, ◖ Researcher ID, ⓘ ORC ID, SNI-CONAHCYT ID or CVU PNPC [No.10 TNRoman]

All ROR-Clarivate-ORCID and CONAHCYT profiles must be hyperlinked to your website.
Prot- ROR University of South Australia • ◖ 7038-2013• ⓘ 0000-0001-6442-4409 • ◉ 416112

Abstract [In English]
Must contain up to 150 words
Graphical abstract [In English]

Authors must provide an original image that clearly represents the article described in the article. Graphical abstracts should be submitted as a separate file. Please note that, as well as each article must be unique. File type: the file types are MS Office files.No additional text, outline or synopsis should be included. Any text or captions must be part of the image file. Do not use unnecessary white space or a "graphic abstract" header within the image file.

Keywords [In English]
Indicate 3 keywords in TNRoman and Bold No. 10

Abstract [In Spanish]
Must contain up to 150 words
Graphical abstract [In Spanish]

Authors must provide an original image that clearly represents the article described in the article. Graphical abstracts should be submitted as a separate file. Please note that, as well as each article must be unique. File type: the file types are MS Office files.No additional text, outline or synopsis should be included. Any text or captions must be part of the image file. Do not use unnecessary white space or a "graphic abstract" header within the image file.

Keywords [In Spanish]
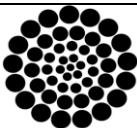Indicate 3 keywords in TNRoman and Bold No. 10

Article

Introduction

Text in TNRoman No.12, single space.

General explanation of the subject and explain why it is important.

What is your added value with respect to other techniques?

Clearly focus each of its features.

Clearly explain the problem to be solved and the central hypothesis.

Explanation of sections Article.

Development of headings and subheadings of the article with subsequent numbers

[Title No.12 in TNRoman, single spaced and bold]

Products in development No.12 TNRoman, single spaced.

Including figures and tables-Editable

In the article content any table and figure should be editable formats that can change size, type and number of letter, for the purposes of edition, these must be high quality, not pixelated and should be noticeable even reducing image scale.

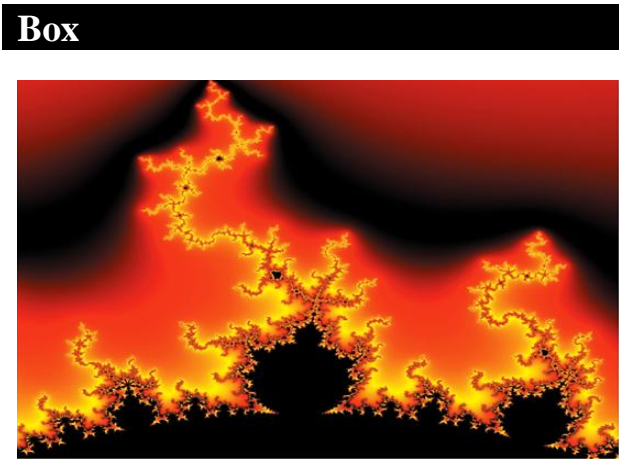[Indicating the title at the bottom with No.10 and Times New Roman Bold]

Box

Figure 1

Title [Should not be images-everything must be editable]
Source [in italic]

Box

Table 1

Title [Should not be images-everything must be editable]

Source [in italic]

The maximum number of Boxes is 10 items

For the use of equations, noted as follows:

$$Y_{ij} = \alpha + \sum_{h=1}^{r} \beta_h X_{hij} + u_j + e_{ij} \qquad [1]$$

Must be editable and number aligned on the right side.

Methodology

Develop give the meaning of the variables in linear writing and important is the comparison of the used criteria.

Results

The results shall be by section of the article.

Conclusions

Clearly explain the results and possibilities of improvement.

Annexes

Tables and adequate sources.
The international standard is 7 pages minimum and 14 pages maximum.

Declarations

Conflict of interest

The authors declare no interest conflict. They have no known competing financial interests or personal relationships that could have appeared to influence the article reported in this article.

Author contribution

Specify the contribution of each researcher in each of the points developed in this research.

Prot-
Benoit-Pauleter, Gerard: Contributed to the project idea, research method and technique.

Availability of data and materials

Indicate the availability of the data obtained in this research.

Funding

Indicate if the research received some financing.

Acknowledgements

Indicate if they were financed by any institution, University or company.

Abbreviations

List abbreviations in alphabetical order.

Prot-
  ANN   Artificial Neural Network

References

Use APA system. Should not be numbered, nor with bullets, however if necessary numbering will be because reference or mention is made somewhere in the Article.

Use the Roman alphabet, all references you have used should be in Roman alphabet, even if you have cited an article, book in any of the official languages of the United Nations [English, French, German, Chinese, Russian, Portuguese, Italian, Spanish, Arabic], you should write the reference in Roman alphabet and not in any of the official languages.

Citations are classified the following categories:

Antecedents. The citation is due to previously published research and orients the citing document within a particular scholarly area.

Basics. The citation is intended to report data sets, methods, concepts and ideas on which the authors of the citing document base their work.

Supports. The citing article reports similar results. It may also refer to similarities in methodology or, in some cases, to the reproduction of results.

Differences. The citing document reports by means of a citation that it has obtained different results to those obtained in the cited document. This may also refer to differences in methodology or differences in sample sizes that affect the results.

Discussions. The citing article cites another study because it is providing a more detailed discussion of the subject matter.

The URL of the resource is activated in the DOI or in the title of the resource.

Prot-
Mandelbrot, B. B. [2020]. Negative dimensions and Hölders, multifractals and their Hölder spectra, and the role of lateral preasymptotics in science. Journal of Fourier Analysis and Applications Special. 409-432.

Intellectual Property Requirements for editing:

- Authentic Signature in Color of Originality Format Author and Coauthors.

- Authentic Signature in Color of the Acceptance Format of Author and Coauthors.

- Authentic Signature in blue color of the Conflict of Interest Format of Author and Co-authors.

Reservation to Editorial Policy

Journal of Experimental Systems reserves the right to make editorial changes required to adapt the Articles to the Editorial Policy of the Research Journal. Once the Article is accepted in its final version, the Research Journal will send the author the proofs for review. ECORFAN® will only accept the correction of errata and errors or omissions arising from the editing process of the Research Journal, reserving in full the copyrights and content dissemination. No deletions, substitutions or additions that alter the formation of the Article will be accepted.

Code of Ethics - Good Practices and Declaration of Solution to Editorial Conflicts

Declaration of Originality and unpublished character of the Article, of Authors, on the obtaining of data and interpretation of results, Acknowledgments, Conflict of interests, Assignment of rights and Distribution

The ECORFAN-Mexico, S.C Management claims to Authors of Articles that its content must be original, unpublished and of Scientific, Technological and Innovation content to be submitted for evaluation.

The Authors signing the Article must be the same that have contributed to its conception, realization and development, as well as obtaining the data, interpreting the results, drafting and reviewing it. The Corresponding Author of the proposed Article will request the form that follows.

Article title:

–   The sending of an Article to Journal of Experimental Systems emanates the commitment of the author not to submit it simultaneously to the consideration of other series publications for it must complement the Format of Originality for its Article, unless it is rejected by the Arbitration Committee, it may be withdrawn.

–   None of the data presented in this article has been plagiarized or invented. The original data are clearly distinguished from those already published. And it is known of the test in PLAGSCAN if a level of plagiarism is detected Positive will not proceed to arbitrate.

–   References are cited on which the information contained in the Article is based, as well as theories and data from other previously published Articles.

–   The authors sign the Format of Authorization for their Article to be disseminated by means that ECORFAN-Mexico, S.C. In its Holding Bolivia considers pertinent for disclosure and diffusion of its Article its Rights of Work.

–   Consent has been obtained from those who have contributed unpublished data obtained through verbal or written communication, and such communication and Authorship are adequately identified.

–   The Author and Co-Authors who sign this work have participated in its planning, design and execution, as well as in the interpretation of the results. They also critically reviewed the paper, approved its final version and agreed with its publication.

–   No signature responsible for the work has been omitted and the criteria of Scientific Authorization are satisfied.

–   The results of this Article have been interpreted objectively. Any results contrary to the point of view of those who sign are exposed and discussed in the Article.

Copyright and Access

The publication of this Article supposes the transfer of the copyright to ECORFAN-Mexico, S.C. in its Holding Bolivia for it Journal of Experimental Systems, which reserves the right to distribute on the Web the published version of the Article and the making available of the Article in This format supposes for its Authors the fulfilment of what is established in the Law of Science and Technology of the United Mexican States, regarding the obligation to allow access to the results of Scientific Research.
Article Title:

Name and Surnames of the Contact Author and the Coauthors	Signature
1.	
2.	
3.	
4.	

Principles of Ethics and Declaration of Solution to Editorial Conflicts

Editor Responsibilities

The Publisher undertakes to guarantee the confidentiality of the evaluation process, it may not disclose to the Arbitrators the identity of the Authors, nor may it reveal the identity of the Arbitrators at any time.

The Editor assumes the responsibility to properly inform the Author of the stage of the editorial process in which the text is sent, as well as the resolutions of Double-Blind Review.

The Editor should evaluate manuscripts and their intellectual content without distinction of race, gender, sexual orientation, religious beliefs, ethnicity, nationality, or the political philosophy of the Authors.

The Editor and his editing team of ECORFAN® Holdings will not disclose any information about Articles submitted to anyone other than the corresponding Author.

The Editor should make fair and impartial decisions and ensure a fair Double-Blind Review.

Responsibilities of the Editorial Board

The description of the peer review processes is made known by the Editorial Board in order that the Authors know what the evaluation criteria are and will always be willing to justify any controversy in the evaluation process. In case of Plagiarism Detection to the Article the Committee notifies the Authors for Violation to the Right of Scientific, Technological and Innovation Authorization.

Responsibilities of the Arbitration Committee

The Arbitrators undertake to notify about any unethical conduct by the Authors and to indicate all the information that may be reason to reject the publication of the Articles. In addition, they must undertake to keep confidential information related to the Articles they evaluate.

Any manuscript received for your arbitration must be treated as confidential, should not be displayed or discussed with other experts, except with the permission of the Editor.

The Arbitrators must be conducted objectively, any personal criticism of the Author is inappropriate.

The Arbitrators must express their points of view with clarity and with valid arguments that contribute to the Scientific, Technological and Innovation of the Author.

The Arbitrators should not evaluate manuscripts in which they have conflicts of interest and have been notified to the Editor before submitting the Article for Double-Blind Review.

Responsibilities of the Authors

Authors must guarantee that their articles are the product of their original work and that the data has been obtained ethically.

Authors must ensure that they have not been previously published or that they are not considered in another serial publication.

Authors must strictly follow the rules for the publication of Defined Articles by the Editorial Board.

The authors have requested that the text in all its forms be an unethical editorial behavior and is unacceptable, consequently, any manuscript that incurs in plagiarism is eliminated and not considered for publication.

Authors should cite publications that have been influential in the nature of the Article submitted to arbitration.

Information services

Indexation - Bases and Repositories

LATINDEX (Scientific Journals of Latin America, Spain and Portugal)
RESEARCH GATE (Germany)
GOOGLE SCHOLAR (Citation indices-Google)
REDIB (Ibero-American Network of Innovation and Scientific Knowledge- CSIC)
MENDELEY (Bibliographic References Manager)
DULCINEA (Spanish scientific journals)
UNIVERSIA (University Library-Madrid)
SHERPA (University of Nottingham - England)
ROAD (Directory of Open Access scholarly Resources)
REBUIN (Network of Spanish University and Scientific Libraries)

Publishing Services

Citation and Index Identification H
Management of Originality Format and Authorization
Testing Article with PLAGSCAN
Article Evaluation
Certificate of Double-Blind Review
Article Edition
Web layout
Indexing and Repository
ArticleTranslation
Article Publication
Certificate of Article
Service Billing

Editorial Policy and Management

21 Santa Lucía, CP-5220. Libertadores -Sucre – Bolivia. Phones: +52 1 55 6159 2296, +52 1 55 1260 0355, +52 1 55 6034 9181; Email: contact@ecorfan.org www.ecorfan.org

Journal of Experimental Systems

"Synthesis and characterization of carbon-based quantum dots for use in biotechnology"

Granados-Olvera, Jorge Alberto, Calvillo-Beltrán, Sofía Valentina, Arroyo-Ordoñez, Ivan and Rangel-Ruíz, Karelia Liliana

Universidad Politécnica de Cuautitlán Izcalli

"Biofilm of potato starch and silver nanoparticles"

Díaz-Silvestre, Sergio E. & Ramirez, Leticia

Universidad Tecnológica de Coahuila

"Solubility study of aerosols and vinyl paint on stone surfaces"

García-Dorado, Samantha, Carranza-Téllez, José, Villegas-Martínez, Rodrigo and García-González, Juan Manuel

Universidad Autónoma de Zacatecas "Francisco García Salinas"

"Anticorrosive SiO_2-PDMS ceramic coating: effect of viscosity and functional group on the siloxane chain"

Salazar-Hernández, Carmen, Salazar-Hernández, Mercedes, Mendoza-Miranda, Juan Manuel and Elorza-Rodríguez, Enrique

Instituto Politécnico Nacional-UPIIG
Universidad de Guanajuato

"Optimization of the finite element meshing for the fabrication of a M3x12x0.5 screw, in 3D printing"

González-Sosa, Jesús Vicente, Avila-Soler, Enrique and Zavala-Osorio, Yadira

Universidad Autónoma Metropolitana

"SiO_2/PDMS modified porous systems for oil removal: reuse cycles studied"

Salazar-Hernández, Carmen, Salazar-Hernández, Mercedes, Mendoza-Miranda, Juan Manuel and León-Reyes, María del Rosario

Instituto Politécnico Nacional-UPIIG
Universidad de Guanajuato